

Copyright © 1985, by the author(s).
All rights reserved.

Permission to make digital or hard copies of all or part of this work for personal or classroom use is granted without fee provided that copies are not made or distributed for profit or commercial advantage and that copies bear this notice and the full citation on the first page. To copy otherwise, to republish, to post on servers or to redistribute to lists, requires prior specific permission.

TRANSFER MAPS AND RETURN MAPS FOR PIECEWISE-LINEAR
THREE-REGION DYNAMICAL SYSTEMS

by

Claus Kahlert and Leon O. Chua

Memorandum No. M85/101

29 November 1985

TRANSFER MAPS AND RETURN MAPS FOR PIECEWISE-LINEAR
THREE-REGION DYNAMICAL SYSTEMS

by

Claus Kahlert and Leon O. Chua

Memorandum No. M85/101

29 November 1985

ELECTRONICS RESEARCH LABORATORY
College of Engineering
University of California, Berkeley
94720

*1.1k
5/20/85*

Transfer Maps and Return Maps for Piecewise-Linear
Three-Region Dynamical Systems*

Claus Kahlert¹ and Leon O. Chua²

¹ Institute for Physical and Theoretical Chemistry,
University of Tübingen, Tübingen, F.R.G.

² Department of Electrical Engineering and Computer Sciences,
University of California, Berkeley, U.S.A.

Abstract

Techniques formerly developed in the theory of Poincaré halfmaps are modified and applied to the three-region piecewise-linear continuous dynamical system of Matsumoto and Chua. Both transfer and return maps, induced by the trajectories inside the intermediate region in state space, are formulated as implicit equations. The boundaries of the domains of these maps are determined explicitly, using the method of calculating the initial points of touching trajectories subject to specific selection rules. A charting of the canonical parameter space of the dynamics that acts on the intermediate region is indicated.

* Research sponsored by the Office of Naval Research Contract N00014-70-C-0572 and National Science Foundation Grant ECS-8313278.

Reprint requests to Dr. C. Kahlert, Institut für Physikalische und Theoretische Chemie der Universität Tübingen, Auf der Morgenstelle 8, D-7400 Tübingen, F.R.G.

1. Introduction

In recent years piecewise-linear autonomous (cf. e.g. [1-5]) and driven (cf. e.g. [6-8]) continuous dynamical systems (specifically with three variables) turned out to be an analytically accessible rich class of systems. On the one hand, piecewise-linear models are used to simplify more general nonlinear systems yielding prototypes for their qualitative dynamical behavior (cf. [9,10]); on the other hand, this class of systems also is directly applicable to some real physical devices, yielding quantitative results (cf. [11,12]).

The simplest three-variable models of interest containing just two regions in state space (that is, two different linear dynamics separated by a plane), can be treated using the theory of Poincaré halfmaps [3], no matter whether the flow is of C^0 or C^1 type, see [3,13] for examples. The system to be discussed in the present paper, taken from [5], possesses three regions and hence two (parallel) separating planes. It represents already the most general example of a whole class of piecewise-linear systems provided that the switching condition is controlled by one variable alone. (This is because for models containing more than three regions, the treatment of the intermediate region as given here can be iterated.) We are going to restrict our attention, however, to the three-region case. In addition, we shall make use of the prototypic symmetry properties of the example system.

In general, when the behavior of the system is governed by more than two different dynamics (three, in the present case), a new type of state space region, not treated in the theory of Poincaré halfmaps, appears: The so called intermediate region, being adjacent to two other regions. For a trajectory entering this region, three ways of dynamical behavior are open in principle. (1) It may remain there forever - if there is an attracting steady state present inside that attracts the trajectory fast enough (other types of limiting structures, like limit cycles, of course cannot appear in a linear, non conservative dynamics); (2) it may pass through (transfer) this region, eventually entering the third region; or, (3) it may instead return to the region it came from. Both, the first and last type of solution may in general also appear for the leftmost and rightmost region, and hence can be treated employing Poincaré halfmaps. However, the second type of behavior is new. We shall develop a formalism for characterizing it.

Fig. 1

Let us, for a moment, forget about the first kind of dynamical behavior mentioned above, as it does not lead to any sort of interesting structures (and, in our present problem, is found for a set of initial conditions of measure zero only). We then have to subdivide the sets of entry points into the intermediate region into those points leading to exit points (for an exact definition of regions, entry points, and exit points see [14]) that are situated inside the other separating plane (via a transferring trajectory), and into those belonging to returning trajectories so that the corresponding exit point lies in the

same plane. These two kinds of orbits induce two types of point transformations (cf. [15] Chapter 31) from one separating plane into the other, or back into the same one, called transfer and return maps.

Calculating the geometrical locus of all initial points of touching trajectories [13,16] in the two separating planes, a technique developed in the theory of Poincaré halfmaps, is again the method of choice in order to determine the boundary between the domains of the present (two) maps. Unfortunately this procedure does not take account of the case of switching dynamics, meaning that additional selection rules [13] have to be introduced in order to pick the physically meaningful solutions.

In this way by classifying the different types of curves that subdivide the separating planes, a charting of the canonical parameter space of the dynamics of the intermediate region can be achieved. This will give more insights into the conditions for the appearance of the double-scroll attractor found in [5] as well as into other chaotic solutions found recently for the same system [17] and a related model [18].

2. Formulation of the Problem

We are going to investigate the following three-variable, three-region piecewise-linear system of C^1 (once continuously differentiable) type:

$$\begin{aligned} \frac{du}{dt} &= -a(f(u) + u - v) \\ \frac{dv}{dt} &= u - v + w \\ \frac{dw}{dt} &= -bv \end{aligned} \quad (1)$$

with the piecewise-straight function

$$f(u) = \begin{cases} n_0 u - n_1 + n_0 & \text{for } u < \delta_- \\ n_1 u & \text{for } \delta_- < u < \delta_+ \\ n_0 u + n_1 - n_0 & \text{for } \delta_+ < u \end{cases} \quad (1a)$$

We leave the function $f(u)$ undefined for $u = \delta_-$ and $u = \delta_+$, respectively, and (as in [14]) determine trajectories at these u values by a limiting process. In the following only the symmetrical case $0 < \delta_+ = \delta_- = -\delta_-$, assumed in [5], will be considered. Since $f(-u) = -f(u)$ and since there is no other nonhomogeneous part at the right-hand side of (1), the whole dynamics possesses the symmetry of the function $f(u)$, i.e., is antisymmetric with respect to the origin. This means that all geometrical and dynamical structures of the state space (except for the origin) have to appear twice (with inverted signs). Note that the shape of $f(u)$, being continuous and antisymmetric, is already the most general possible one [19].

Adopting the notation of [13], we first of all find that the state space T is, like the function $f(u)$, subdivided into three parts (called regions):

and

$$\begin{aligned}
 T_- &:= \{(u,v,w)^T \mid u < -\delta\} , \\
 T_0 &:= \{(u,v,w)^T \mid -\delta < u < \delta\} , \\
 T_+ &:= \{(u,v,w)^T \mid \delta < u\} ,
 \end{aligned}
 \tag{2}$$

with the two separating planes

and

$$\begin{aligned}
 S_- &:= \{(u,v,w)^T \mid u = -\delta\} \\
 S_+ &:= \{(u,v,w)^T \mid u = \delta\} ,
 \end{aligned}
 \tag{3}$$

respectively.

The steady states of the three partial dynamics are easily found to be located at

$$L_- = \begin{pmatrix} -k \\ 0 \\ k \end{pmatrix}, \quad L_0 = \begin{pmatrix} 0 \\ 0 \\ 0 \end{pmatrix}, \quad L_+ = \begin{pmatrix} k \\ 0 \\ -k \end{pmatrix}, \tag{4}$$

where

$$k := \frac{n_0 - n_1}{n_0 + 1}, \tag{4a}$$

cf. [5]. This immediately implies that L_0 is a real steady state [20] for all values of the system parameters. The two others (L_- and L_+) are real steady states (located inside T_- or T_+ , respectively) for $k > \delta$ and are virtual steady states [20] otherwise. For $|k| < \delta$ all three steady states are located inside T_0 , while for $k < -\delta$, L_+ (the steady state governing the dynamics of T_+) is found inside the region T_- while L_- (for reasons of symmetry), is situated inside T_+ .

For determining the domains of the transfer and return maps inside the separating planes, only the dynamics of the intermediate region T_0 is relevant. In the following, we therefore treat this region and its dynamics alone. As we are left with just one dynamics, up till Section 4, we shall suppress the index "0" (indicating the pertinent dynamics) for the quantities occurring (like the eigenvalues, for example).

Inside the region T_0 , the equation of motion can be written as a homogeneous linear differential equation

$$\frac{d}{dt} \mathbf{l} = \mathbf{B}\mathbf{l} \tag{5}$$

with the state vector $\mathbf{l} := (u, v, w)^T$ and the dynamical matrix

$$\mathbf{B} := \begin{pmatrix} -a(n_1+1) & a & 0 \\ 1 & -1 & 1 \\ 0 & -b & 0 \end{pmatrix}. \tag{5a}$$

The eigenvalues λ_i ($i=1,2,3$) of this matrix are solutions of the characteristic equation

$$\lambda^3 - \lambda^2 \text{tr } \mathbf{B} + \lambda \text{min } \mathbf{B} - \det \mathbf{B} = 0, \tag{6}$$

where the trace, the principal minors, and the determinant of the matrix \mathbf{B} (all being invariants) are:

$$\begin{aligned} \text{tr } B &= -a(n_1+1)-1 = \lambda_1 + \lambda_2 + \lambda_3, \\ \text{min } B &= b+an_1 = \lambda_1\lambda_2 + \lambda_1\lambda_3 + \lambda_2\lambda_3, \\ \text{det } B &= -ab(n_1+1) = \lambda_1\lambda_2\lambda_3. \end{aligned} \quad (6a)$$

and

Equation (6) can be solved analytically using Cardano's formula; this procedure will, however, be omitted here since it is standard and yields no new insights into the structure of the problem. One set of parameter values leading to the double-scroll attractor is given in [5]. For this set ($a=9$, $b=14\frac{2}{7}$, $n_0=-5/7$, and $n_1=-8/7$; $k=3/2$), one real positive eigenvalue (λ_1) and two complex conjugate eigenvalues with negative real part (λ_2, λ_3) are found for the dynamics of T_0 . Thus the steady state L_0 possesses saddle-focus character. We are going to take this property as a prerequisite in our further discussion.

As to the eigenvectors of the dynamical matrix B , they are found to be

$$t^i = \begin{pmatrix} 1 \\ \frac{\lambda_i}{a} + n_1 + 1 \\ \frac{-b}{\lambda_i} \left(\frac{\lambda_i}{a} + n_1 + 1 \right) \end{pmatrix}. \quad (7)$$

The eigenvectors determine the transformation matrix

$$|H| := (t^1, t^2, t^3) \quad (8)$$

which diagonalizes B :

$$\mathcal{A} := \mathbb{H}^{-1} \mathbb{B} \mathbb{H} = \begin{pmatrix} \lambda_1 & 0 & 0 \\ 0 & \lambda_2 & 0 \\ 0 & 0 & \lambda_3 \end{pmatrix} . \quad (9)$$

We left the eigenvectors unnormalized. So in the first row of \mathbb{H} (which gives the transformation to the u variable, the one controlling the switching of the dynamics) only "1's" appear. This yields a more transparent representation of our subsequent results. (See [13] for related expressions using normalized eigenvectors.)

The equation of motion, written in diagonalized coordinates (in k -space, taking the eigenvectors (7) as a basis, with coordinates x , y , and z), then reads

$$\frac{d}{dt} \begin{pmatrix} x \\ y \\ z \end{pmatrix} = \frac{d}{dt} k = \mathcal{A} k . \quad (10)$$

As was shown in [13], the dynamics of the system can be formulated in the space $\mathbb{R} \times \mathbb{C}$ (rather than $\mathbb{R} \times \mathbb{C}^2$, cf. also [21]) by introducing a new metrics and dropping the side condition ($z = \bar{y}$). Further on, by a nonsingular transformation of time (stretching by a factor of $|\operatorname{Re} \lambda_2|$), the equation of motion in reduced, diagonalized coordinates x and y (with $x \in \mathbb{R}$ and $y \in \mathbb{C}$) becomes simply:

$$\begin{aligned} \frac{dx}{dt} &= \rho x \\ \text{and} \quad \frac{dy}{dt} &= (-1 + i\omega)y , \end{aligned} \quad (11)$$

whereby the canonical parameters [13]

$$\xi := \left| \frac{\lambda_1}{\operatorname{Re} \lambda_2} \right| > 0 \quad \text{and} \quad \omega := \left| \frac{\operatorname{Im} \lambda_2}{\operatorname{Re} \lambda_2} \right| > 0 \quad (11a)$$

were used.

Thus, after an (in parameter space) local gauging process [13], ξ is the growth factor in the direction of the real eigenvector while ω is the angular frequency of the focal motion (with shrinking amplitude in positive time).

The two switching conditions $|u| = \delta$ read in x, y coordinates:

$$x + 2y = \pm \delta, \quad (12)$$

where the complex variable y was written as $\eta + i\xi$ ($\eta, \xi \in \mathbb{R}$). This (Eqs. 11 and 12) is our final representation of the problem. Only the equation of motion (11) together with the switching condition (12) will be treated further on.

Let us now investigate how the dynamics of the system produces further geometrical structures inside the two separating planes S_{\pm} . For reasons of symmetry it suffices to treat just one of these two planes. We are going to choose S_{-} . (All results carry over to S_{+} by a change of sign in all coordinates.)

In x, y coordinates, the separating plane S_+ is given by (12) using the "-" sign: i.e., every point inside this plane is characterized by its x and y coordinates, while the value of η is a linear function of x alone:

$$\eta_-(x) := -\frac{\delta + x}{2} . \quad (13)$$

An analogous expression holds true for the plane S_- (with the sign of δ changed).

An additional geometrical property comes from the dynamics of the system: it divides the separating plane S_+ into two halves:

$$\begin{aligned} S_+^+ &:= \{(u, v, w)^T | u = -\delta, \dot{u}_{S_+} > 0\} \\ \text{and} \\ S_+^- &:= \{(u, v, w)^T | u = -\delta, \dot{u}_{S_+} < 0\} , \end{aligned} \quad (14)$$

Here \dot{u}_{S_+} is the derivative of u with respect to t , taken inside S_+ :

$$\begin{aligned} \dot{u}_{S_+} &:= \left. \frac{du}{dt} \right|_{S_+} = \xi x + 2\text{Re}[(-1+i\omega)(\eta_-(x)+i\zeta)] \\ &= (\xi+1)x + \delta - 2\omega\zeta . \end{aligned} \quad (15)$$

In between these two halfplanes there is found a separating straight line

$$W_- := \{(u, v, w)^T | u = -d, \dot{u}_- = 0\} ; \quad (16)$$

it can be written in x, ξ coordinates as

$$\xi_{u_-}(x) = \frac{d + (\xi + 1)x}{2\omega} \quad (16a)$$

by setting the right-hand side of (15) equal to zero (cf. [13] for a related expression). Inside the halfplane S_-^+ , trajectories always cross the separating plane from T_- towards T_+ , while inside S_-^- the systems runs in the opposite direction. Along the straight line W_- , and of course along W_+ too, the trajectories are tangential to S_- or S_+ , respectively.

The character of the u extrema of the trajectories along the line W_- can be determined by calculating the second derivative of u with respect to t , along W_- .

$$\begin{aligned} \ddot{u}_- &:= \left. \frac{d^2 u}{dt^2} \right|_{u_-} = \xi^2 x + 2\text{Re}[(-1+i\omega)^2(\eta_-(x) + i\xi_{u_-}(x))] \\ &= x((\xi + 1)^2 + \omega^2) + d(\omega^2 + 1) . \end{aligned} \quad (17)$$

Hence there exists a point on W_- with x coordinate

$$x_{u_-} = -d \frac{\omega^2 + 1}{(\xi + 1)^2 + \omega^2} , \quad (18a)$$

and ξ coordinate

$$\xi_{u_-}(x_{u_-}) = \frac{d}{2\omega} \frac{\xi(\xi + 1 - \omega^2)}{(\xi + 1)^2 + \omega^2} , \quad (18b)$$

where the curvature of the trajectory at its extremal u value vanishes (cf. [22] for an analogous result). At this point (going along W_+), the extremum changes its character. For x values greater than x_* the trajectories possess a minimum of u at the points of W_+ , while for smaller values of x we find maxima of the u components on the orbits.

Fig. 2

Since for any bounded initial point a unique solution of the system exists, due to the C^1 character of the flow (the derivatives with respect to t match inside the separating planes S_\pm), the above results could be found by looking just at the dynamics acting on T_+ , without considering the regions T_- and T_+ .

We are now in the position to define transfer and return maps on the separating plane S_- . A trajectory entering T_+ in a point of S_-^+ may either leave this region again by crossing the same separating plane (returning to T_+) or by crossing the other plane S_+ , eventually entering T_- (transferring). Hence the dynamics of T_+ induces two different types of maps. A transfer map (with range inside S_+),

$$\mathcal{T} : S_-^+ \rightarrow S_+^+; (x, f) \mapsto \mathcal{T}(x, f) \quad , \quad (19a)$$

and a return map (with range inside S_-),

$$\mathcal{R} : S_-^+ \rightarrow S_-^+; (x, f) \mapsto \mathcal{R}(x, f) \quad . \quad (19b)$$

A concrete, implicit representation of these two maps can be obtained by inserting the solution of the linear differential equation (11) with initial point $(x, \eta_-(x) + i\xi)^T$ in S_+ into the switching conditions, i.e., by calculating the u component of the trajectory with the above initial condition, namely,

$$u(t) = xe^{st} + 2\text{Re}[(\eta_-(x) + i\xi)e^{(-1+i\omega)t}] \quad , \quad (20)$$

and requiring $u(\tau_\pm) = \pm\delta$ [13]. This yields:

$$xe^{s\tau_+} + 2\text{Re}[(\eta_-(x) + i\xi)e^{(-1+i\omega)\tau_+}] = \delta \quad , \quad (21a)$$

and

$$xe^{s\tau_-} + 2\text{Re}[(\eta_-(x) + i\xi)e^{(-1+i\omega)\tau_-}] = -\delta \quad . \quad (21b)$$

Equation (21a) is valid for the transfer map \mathcal{T} while (21b) is the one that applies for the return map \mathcal{R} . Note that these equations differ only by the signs of δ on the two right-hand sides.

The two expressions (21a) and (21b) are scalar, transcendental implicit equations for the time at which the trajectory fulfills the switching condition $u = \delta$ or $u = -\delta$, respectively. Thus

$$\begin{aligned} \mathcal{T}(x, \xi) &= (xe^{s\tau_+}, (\eta_-(x) + i\xi)e^{(-1+i\omega)\tau_+})^T \\ \mathcal{R}(x, \xi) &= (xe^{s\tau_-}, (\eta_-(x) + i\xi)e^{(-1+i\omega)\tau_-})^T \end{aligned} \quad (22)$$

For finite values of the entry coordinates x and ξ , the equations (21a) and (21b) both yield a countable infinity of

negative solutions (τ values) [16], but there are either no or at most a finite number of solutions found on the positive half-line \mathbb{R}^+ . This is a direct consequence of the "Lemma from Analysis", shown in the Appendix. To apply it, we just have to estimate the exponentially decreasing amplitude of the oscillatory term by the constant $2\sqrt{\eta_-^2(x) + \xi^2}$ (that is the value at $t=0$) and do an appropriate shift and rescaling of both time (by a factor of $1/\xi$) and amplitude (by a factor of $1/x$).

The only physically meaningful solution, for both x and ξ given, is the smallest positive solution found for either of the two equations. This corresponds to the first time that the trajectory with initial condition $(x, \eta_-(x) + i\xi)^T$ meets the requirements of one of the switching conditions, provided there is any positive solution at all present. Otherwise, the system is attracted by the steady state L_0 and hence remains forever inside the region T_0 .

3. The Domains of the Transfer and the Return Map

3.1. General Properties

If all (positive) solutions of the implicit equations (21a) and (21b) could be found for arbitrary finite values of x and ξ , it would be easy to determine the domains of the transfer and return map, respectively, by just selecting the smallest positive solution of both equations. Unfortunately these

transcendental equations cannot be solved analytically. So we have to apply a different approach in order to obtain a result in closed form.

Let us first discuss the properties of the statical and dynamical manifolds [13] that correspond to the dynamics of T_0 . The stable manifold M_s (meaning that perturbations off this manifold are damped away by the dynamics of the system) of the steady state L_0 is spanned by the real eigenvector t^1 alone. This manifold intersects the two separating planes S_{\pm} in the points $h_{\pm} = (x_{0\pm}, 0)^T$, with

$$x_{0\pm} := \pm \delta, \quad (23a)$$

where the "+" applies for the intersection with S_+ and the "-" for the one with S_- . This simple form is a consequence of (12) (and hence the lack of normalisation of the eigenvectors).

The unstable manifold M_u (unstable in the sense that perturbations off this manifold are amplified by the dynamics) is the focal plane of the steady state L_0 . This manifold intersects the two separating planes in two straight lines Z_{\pm} characterized by $x=0$ and $\eta = \eta_{0\pm}$ or η_{\pm} , respectively, with

$$\eta_{0\pm} := \pm \frac{\delta}{2}, \quad (23b)$$

cf. again (12).

The statical manifolds mentioned are limiting cases of more general, so called dynamical manifolds \mathcal{M} , cf. [13]. These manifolds are constructed by taking all points of all trajectories (for positive and negative times) that differ in their initial conditions by just a phase (of the initial y coordinate), without considering the switching of dynamics, i.e., they are confined to one dynamics. The geometric shapes of the dynamical manifolds are logarithmic double-cones, with the one-dimensional (in this case stable) manifold behaving as an axis of rotational symmetry, and the two-dimensional (in this case unstable) manifold being the separating plane between the two branches. By construction, corresponding entry and exit points of the region T_0 must be situated on the intersection curves of one of the separating planes with the pertinent dynamical manifold. As there are two separating planes present for T_0 , however, both intersecting this manifold, the dynamics need not map an entry point into the same plane and hence onto the same intersection curve, as it was the case for two-region systems [3,13].

Fig. 3

Employing the classification used in [3], the types of intersection curves appearing inside S_1 are Ω -curves, Cartesian leaves, and isolae with base lines, valid for the halfplane $x < 0$, while only Ω -curves appear for $x > 0$. Inside the other separating plane, S_2 , we find the same situation with the signs of x interchanged. Again the curve $\omega^2 = \xi + 1$ [13] inside the canonical parameter space of the dynamics from T_0 marks the

boundary for the appearance of complicated isolae [3]. (For a detailed discussion of complicated isolae and their importance for the maps induced, see [13,22].)

3.2. The Line $x=0$

Let us now investigate the implications of the structures discussed above for the solutions of the implicit equations (21a) and (21b). First of all we find:

THEOREM 1 For $x \neq 0$ there is at least one solution of either (21a) or (21b) present inside the positive halfline \mathbb{R}^+ . ***

PROOF Due to the symmetry of the problem, we can assume $x > 0$ without loss of generality. In this case at least one solution can be demonstrated.

For a trajectory starting at the initial point $(x, \eta_-(x) + i\xi)^T$ we know from (20)

$$u(0) = x + 2\eta_-(x) = -\delta . \tag{24}$$

Let us first treat the case $x < \delta$. If we choose

$$t_1 = \frac{1}{\xi} \ln \frac{x + \delta}{x} , \tag{25}$$

then, after the time t_1 , the u component of the trajectory arrives at

$$u(t_1) = xe^{st_1} + 2e^{-t_1}[\eta_-(x)\cos\omega t_1 - \int \sin\omega t_1] \quad (26a)$$

The first term of (26a) now by construction has reached the value $x_{**} = \delta$ (Fig. 3), while the influence of the second (oscillatory) term is still unknown. This term, however, certainly vanishes at a time t_2 inside the interval $[t_1, t_1 + \pi/\omega]$, so that we find:

$$u(t_2) = xe^{st_2} \gg xe^{st_1} = \delta > -\delta = u(0) \quad (26b)$$

Since $u(t)$ is continuous everywhere, the intermediate value theorem (Bolzano) applies, proving the existence of a τ with $u(\tau) = \delta$.

If now $x \gg \delta$, we can choose $t_1 = 0$ and (26b) is now changed to

$$u(t_2) = xe^{st_2} \gg x \gg \delta > -\delta = u(0) \quad (27)$$

while all the other arguments carry through unchanged. **Q.E.D.**

This theorem reflects the fact that L_0 , the steady state at the origin of the state space, is of saddle-focus type and hence cannot attract any trajectory unless the system enters the region T_0 inside the unstable manifold M_u (characterized by

$x=0$). Remains the question for which initial values of ξ the latter possibility is realized, so that no positive solution, neither of (21a) nor of (21b), exists.

Inside the unstable manifold M_u all trajectories starting in a point of Σ_- are of the form

$$y(t) = (\eta_- + i\xi) e^{(-1 + i\omega)t} , \quad (28)$$

i.e., the orbits are shrinking exponential spirals. Writing them in polar coordinates with $R(t) = |y(t)|$ the radius and $\chi(t) = \arg y(t)$ the phase of $y(t)$, we find:

and

$$\begin{aligned} R(t) &= R_0 e^{-t} \\ \chi(t) &= \chi_0 + \omega t \end{aligned} \quad (29)$$

where

$$R_0 := R(0) = \sqrt{\eta_-^2 + \xi^2}$$

and

$$\chi_0 := \chi(0) = \pi - \arctan \frac{\xi}{\eta_-} . \quad (29a)$$

We now need some results from [16] concerning the properties of flat spirals like (28). First of all the extremal u values of the trajectories in question are found at the phases $\chi_{max} = -\arctan 1/\omega + 2\pi n$ (maximum) and at $\chi_{min} = \pi - \arctan 1/\omega + 2\pi n$ (minimum), where n is any nonnegative integer. So an easy criterion whether a trajectory can fulfill the switching conditions (21a) is to calculate its maximal u value. This yields the condition:

$$u(t_{\text{opt}}) = R_0 \cos \chi_{\text{opt}} \exp(-t_{\text{opt}}) > \delta \quad (30)$$

with

$$t_{\text{opt}} = \frac{\chi_{\text{opt}} - \chi_0}{\omega} \quad (30a)$$

It suffices to treat this case, since χ_{opt} is always smaller than χ_0 by a amount of π . Hence for a flat shrinking spiral, starting at an u value of $-\delta$, the switching condition cannot be fulfilled for positive times at $u = -\delta$ if it is not satisfied at $u = \delta$ for an earlier time; if, on the other hand, this is the case, the smallest solution of (21a) and (21b) has already been found.

A critical situation is reached for an initial $\xi = \xi_0$ leading to $u(t_{\text{opt}}) = \delta$. For all possible initial points (from Σ) with $|\xi|$ smaller than this given one, no positive solution of (21a), and hence of (21b) too, appears, while for all absolute values of ξ greater than this given one, the entry points lead to transferring trajectories, i.e., these points belong to $\mathcal{D}(\mathcal{T})$ the domain of the transfer map \mathcal{T} .

A concrete calculation of the critical ξ value means to solve the equation

$$u(t_{\text{opt}}) = R_0 \cos \chi_{\text{opt}} \exp(-t_{\text{opt}}) = \delta \quad (31)$$

for R_0 . This, however, is impossible in closed form, since t_{opt} itself is (via χ_0 , cf. (30a)) a function of R_0 . As was shown

in [16], R_0 is a fixed point of the function

$$F^-(R) = a \exp\left(-\frac{1}{\omega} \arctan \frac{\sqrt{R^2 - \eta_0^2}}{\eta_0}\right), \quad (32)$$

where

$$a = \frac{\eta_0}{\omega} \sqrt{\omega^2 + 1} \exp\left(\frac{1}{\omega} (\pi - \arctan \frac{1}{\omega})\right). \quad (32a)$$

This fixed point is stable for all values of $\omega > 0$, as can be tested immediately by the criterion, [16],

$$F^-(\hat{R}) > \hat{R} \quad (33)$$

with

$$\hat{R} := \frac{\eta_0}{\omega} \sqrt{\omega^2 + 1}, \quad (33a)$$

yielding:

$$F^-(\hat{R}) = \hat{R} \exp\left(\frac{1}{\omega} (\pi - 2 \arctan \frac{1}{\omega})\right). \quad (34)$$

Since $0 < \omega < \infty$ one always finds $0 < \arctan 1/\omega < \pi/2$, and hence the numerical value of the exponential in (34) is greater than 1 for all possible values of ω , proving stability of the fixed point.

As far as the numerical properties are concerned, the above mentioned fixed point algorithm converges rather fast. In addition, luckily \hat{R} in all cases is contained inside the basin of attraction of the fixed point, meaning that this point is an

universal initial point for the fixed point iteration. If $F^-(\hat{R})$ comes close to \hat{R} itself, however, the speed of convergence drops rapidly. (For this, analytically known, fixed point we find $dF^-(\hat{R})/dR = -1$, i.e., it is indifferently stable.) Due to the fact that $dF^-/dR < 0$ at all fixed points of the function F^- [16], these points are always approached on an alternating orbit. So the convergence can be improved considerably (for small values of ω up to a factor of 10^6 and more) and may be even made possible in numerical practice, by using

$$R_{i+1} = F^-(R_i) + d(R_i - F^-(R_i)) \tag{35a}$$

for the fixed point iteration instead of the ordinary

$$R_{i+1} = F^-(R_i) \tag{35b}$$

formula.

The d in (35a) is a damping factor that should be taken from a range of about 0.2 to 0.8 in order to obtain good results.

Now it is easy to determine the basin of attraction of the saddle-focus L_0 . One end point of this range is the intersection of Σ_- and W_- , yielding the ξ value $\delta/2\omega$, cf. (16a). So the range in question is just the open interval $(\xi_0, \delta/2\omega)$ (where $\xi_0 := -\sqrt{R_0^2 - \gamma_0^2}$) on the straight line Σ_- . Only for these entry points with exactly vanishing x component (a structurally unstable situation) the system remains forever inside T_0 ,

converging towards the steady state L_0 .

3.3. The Range $x > 0$

After having classified the line Σ of the separating plane S , let us now turn to values of x greater than zero. For this portion we find:

THEOREM 2 All entry points of T_0 situated inside S with $x > 0$ are initial points of transferring trajectories. ***

PROOF This proof is similar to that for Theorem 1. We have to investigate the behavior of the u component of the trajectory, i.e., the function $u(t)$, cf. (20). Let us first suppose the switching condition (21b) to be fulfilled for some τ_2 . To abbreviate the notation, we decompose $u(t)$ into an exponentially growing term $e(t) := xe^{\delta t} > 0$ and an oscillatory term $o(t) := \eta_-(x) \cos \omega t - \int \sin \omega t$ with an exponentially decreasing amplitude $a(t) := 2e^{-\delta t} > 0$. Then at τ_2 , where (21b) is fulfilled, by construction the following inequality holds true:

$$\begin{aligned} u(\tau_2) &= e(\tau_2) + a(\tau_2)o(\tau_2) = -\delta = u(0) \\ a(\tau_2)o(\tau_2) &= -\delta - e(\tau_2) \\ a(\tau_2)o(\tau_2) &< -\delta \end{aligned} \tag{36}$$

Now for $t_1 := \tau_2 - \pi/\omega > 0$ the amplitudes show $a(t_1) > a(\tau_2)$ while the oscillatory term just changes its sign $o(t_1) = -o(\tau_2)$, hence

$$a(t_1) \circ(t_1) > \delta . \quad (37)$$

But since $e(t) > 0$ for all values of t , to obtain $u(t_1)$ from the left-hand side of (37) we have to add a positive quantity to the product $a(t_1) \circ(t_1)$. Hence $u(t_1)$ too is certainly greater than δ . So, by the intermediate value theorem there exists a solution τ_1 of (21a) inside the open interval $(0, t_1)$. This shows that for initial points from the halfplane $x > 0$, for every positive solution τ_2 of (21b) a corresponding positive solution of (21a) can be found that is smaller than $\tau_2 - \pi/\omega$.

If, on the other hand, there is no positive solution of (21b) present, then the solution guaranteed by Theorem 1 (since $x \neq 0$) has to be a solution of (21a). Q.E.D.

This theorem shows that for $x > 0$ the first positive solution of the equation $|u(t)| = \delta$ always fulfills (21a), meaning that no returning trajectories with initial x coordinates greater than zero appear. It also reflects the fact that for the upper half plane only Ω -curves are found as intersections of dynamical manifolds with S_+ .

3.4. The Range $x < 0$

Now, as the remaining main problem we have to treat the portion of S_+ possessing $x < 0$. There we cannot use the above arguments (with changed signs inside S_+) because only the

function $e(t)$ is antisymmetric with respect to x , whereas $a(t)$ behaves independently of x and $o(t)$ is a nonhomogeneous linear function of this initial coordinate.

Inside the mentioned portion of S^* we meet both transferring and returning trajectories. To visualize this situation, first imagine an entry point with x value less than x_w (cf. (15b)) and an initial f close to $f_w(x)$ (cf. (14b)). Since the maximal u value of a trajectory continuously depends on the initial condition, there is a strip of entry points to the left of the straight line W leading to maximal u values of the trajectories from the interval $(-\delta, -\delta+\epsilon)$. Since these values are less than δ , those initial points certainly give rise to returning trajectories.

On the other hand we can choose $|f|$ and simultaneously the initial amplitude (being $2\sqrt{\eta^2(x)+f^2}$) big enough such that at $t_1 := \pi/2\omega$ the following condition

$$u(t_1) = xe^{3t_1} - 2e^{-t_1}f > \delta \quad (38)$$

is fulfilled. This equation can easily be solved for f , yielding:

$$-f > e^{t_1} \frac{\delta - xe^{3t_1}}{2} . \quad (38a)$$

Since the u maximum of the trajectories in general is not located at the phase $\chi_0 + \pi/2$, all \int fulfilling (38a) are certainly situated inside $\mathcal{D}(\mathcal{T})$ the domain of the transfer map \mathcal{T} . So we now have found examples for both types of initial points (leading to transferring and to returning trajectories, respectively, cf. Fig. 5).

Fig. 5

A similar argument can be used to show the following

THEOREM 3 For $x < 0$ all transferring trajectories intersect the plane S , for a time $\tau < 2\pi/\omega$. ***

This means that a solution that does not intersect S , during the first turn around the stable manifold is a returning trajectory. This theorem is again a consequence of the fact that inside S , for $x < 0$ only Ω -curves appear.

PROOF Let the first u -maximum of the trajectory in question be located at $t_1 < 2\pi/\omega$. If there occurs no intersection during this turn, i.e., $u(t_1) < \delta$, then for the next maximum at t_2 we find, due to the maximum property of $u(t)$, $o(t_2) > 0$,

$$a(t_2) < a(t_1) \quad . \quad (39a)$$

We can therefore employ the Lemma of the Appendix to estimate

$$u(t_2) = e(t_2) + a(t_2)o(t_2) < e(t_2) + a(t_1)o(t_2) \quad . \quad (39b)$$

This yields $u(t_2) < u(t_1) < \delta$. The above process may be iterated, showing that all subsequent u maxima are smaller than δ too. Since $x \neq 0$, Theorem 1 guarantees at least one solution. In the present case, this must be a solution of (21b), i.e., a re-turning trajectory. Q.E.D.

The preceding arguments show how to find the boundary between the domains of the transfer and the return map. A limiting case is reached when the first u maximum of a trajectory exactly reaches the value δ , i.e., when the trajectory touches the plane S_0 in a point of the line W_0 . These points are certainly maxima of the u component of the trajectories since their x values are less than zero and, on the other hand, x_{00} is positive. So the trajectory has to fulfill (21a) while simultaneously the derivative of u with respect to t must vanish at this point:

$$\xi x e^{\omega t} - 2e^{-T} [(\eta_-(x) + \omega f) \cos \omega t + (\omega \eta_-(x) - f) \sin \omega t] = 0 \quad (40)$$

Compare (15) for a similar condition on the initial points inside S_0 .

Now we have to calculate the entry points that are initial values for the last-mentioned type of orbits, called touching trajectories. This procedure was developed in principle in [16,22]. Since we cannot analytically solve (21a) alone, it is also not possible to solve it simultaneously with (40); so we have to adopt a different approach.

First of all let us think of the whole state space being governed by the dynamics of T_0 only; i.e., for the moment we ignore the switching of dynamics. Secondly, we formulate an inverse problem. To do this let us look for the geometric locus of all initial points of trajectories fulfilling the switching condition $u=\delta$ after a certain, fixed amount of time. For this purpose we rewrite (21a) using the definition of $\eta_-(x)$:

$$xe^{\omega T} - 2e^{-T} \left[\frac{\delta+x}{2} \cos \omega T + \xi \sin \omega T \right] = \delta \quad , \quad (41)$$

and solve for ξ , yielding the function $\xi_T(x)$ (being linear in x):

$$\xi_T(x) = \frac{e^{\omega T} - \cos \omega T}{2 \sin \omega T} x - \frac{e^T + \cos \omega T}{2 \sin \omega T} \delta \quad . \quad (42)$$

So the curves of equal mapping durations [16,22] are simply straight lines inside the separating plane S_0 .

Note that in contrast to the $\xi_T(x)$ found in [16,22], which reproduces the equation for W_0 as T goes to zero, here the second term of the expression (42) diverges in the same limit. This singularity reflects the fact that for finite values of the initial coordinate ξ no transfer through the region T_0 can happen in no time. However, if $|\xi|$ itself goes to infinity, written in cylindrical coordinates, it becomes clear that the phase difference and hence the mapping time between the entry point and the exit point shrinks to zero.

The lines $f_{\tau}(x)$ are not parallel for different values of τ , i.e., they may intersect each other. Such an intersection point (say of $f_{\tau_1}(x)$ and $f_{\tau_2}(x)$) means that the trajectory starting there fulfills the switching condition (without actually switching through) at time τ_1 and thereafter at time τ_2 . Certainly the second solution, τ_2 , is an artifact due to the assumption of a homogeneous dynamics acting on the whole state space. However, if we think of τ_1 being the first and τ_2 the second solution of (21a) and if we decrease the interval length

$$\Delta\tau := \tau_2 - \tau_1, \quad (43)$$

i.e., the time the trajectory runs inside the region T , under the dynamics of T_0 , then in the limit for $\Delta\tau \rightarrow 0$ we find a touching trajectory (cf. Fig. 7). So we have to calculate the intersection points of the straight lines $f_{\tau}(x)$ and $f_{\tau+\Delta\tau}(x)$, i.e., to solve the equation

Fig. 7

$$f_{\tau}(x) = f_{\tau+\Delta\tau}(x) \quad (44)$$

and then take the limit $\Delta\tau \rightarrow 0$ of this expression (cf. Fig. 8).

For $x_{\tau, \Delta\tau}$, the x component of the intersection point, we find, using $x_{0^*} = \delta$:

$$\begin{aligned} & x_{\tau, \Delta\tau} \left[\frac{e^{(\delta+1)\tau} - \cos\omega\tau}{2\sin\omega\tau} - \frac{e^{(\delta+1)(\tau+\Delta\tau)} \cos\omega(\tau+\Delta\tau)}{2\sin\omega(\tau+\Delta\tau)} \right] \\ &= x_{0^*} \left[\frac{e^{\tau} + \cos\omega\tau}{2\sin\omega\tau} - \frac{e^{\tau+\Delta\tau} + \cos\omega(\tau+\Delta\tau)}{2\sin\omega(\tau+\Delta\tau)} \right] \end{aligned} \quad (45)$$

This can be solved for $x_{T,\Delta T}/x_{0^*}$ yielding:

$$\frac{x_{T,\Delta T}}{x_{0^*}} = \frac{Z_T(\Delta T)}{N_T(\Delta T)} \quad (46)$$

with

$$Z_T(\Delta T) = \sin\omega(T+\Delta T)(e^T + \cos\omega T) - \sin\omega T(e^{T+\Delta T} + \cos\omega(T+\Delta T))$$

and

(46a)

$$N_T(\Delta T) = \sin\omega(T+\Delta T)(e^{(s+1)T} - \cos\omega T) - \sin\omega T(e^{(s+1)(T+\Delta T)} - \cos\omega(T+\Delta T)).$$

Fig. 8

Unfortunately both functions $Z_T(\Delta T)$ and $N_T(\Delta T)$ vanish at the origin, so the expression for $x_{T,\Delta T}/x_{0^*}$ is undefined as ΔT goes to zero. Since both functions approach zero linearly, the limit can, however, be taken regularly by using l'Hospital's rule, i.e., investigating the limits of the derivatives

$$z(\tau) := \lim_{\Delta T \rightarrow 0} \frac{d}{d\Delta T} Z_T(\Delta T) = \omega + e^T(\omega \cos\omega T - \sin\omega T) \quad (47a)$$

and

$$n(\tau) := \lim_{\Delta T \rightarrow 0} \frac{d}{d\Delta T} N_T(\Delta T) = -\omega + e^{(s+1)T}(\omega \cos\omega T - (s+1)\sin\omega T). \quad (47b)$$

This quotient remains finite for $\tau > 0$ and hence yields an analytical expression for the x components of the entry points of touching trajectories:

$$x_\tau := \lim_{\Delta T \rightarrow 0} x_{T,\Delta T} = x_{0^*} \frac{z(\tau)}{n(\tau)}. \quad (48)$$

Now the ξ components of these points are easily found by inserting x_τ into (42). This is the main result of the present paper: We have found a parameter representation of the boundary

curve $P(\tau)$ in the (system independent) x, ξ representation of the plane S_+ :

$$P(\tau) := (x_\tau, \xi_\tau(x_\tau))^\tau \quad (49)$$

Comparing this to analogous expressions for $\xi_\tau(x_\tau)$ in [16,22], we find only a different sign for the ω and the $\sin\omega\tau$ terms in the expression for $z(\tau)$ while in $n(\tau)$ only the sign of the $\sin\omega\tau$ term is changed. These changes of signs, however, result in the existence or nonexistence of the limits $\tau \rightarrow 0$ and $\tau \rightarrow \infty$. For $\tau \rightarrow 0$ (48) diverges like (42). Expanding $n(\tau)$ at the origin up to second order yields

$$n(\tau) = -\frac{\tau^2}{2} \omega((\xi+1)^2 + \omega^2) + O(\tau^3) \quad , \quad (50)$$

i.e., there is a second order singularity of x_τ at the origin.

This means that there is no finite entry point leading to a touching trajectory with mapping time zero. This is an obvious result, if we keep in mind that there is no transfer in no time through T_0 for finite initial coordinates. The other limiting case, $\tau \rightarrow \infty$, simply yields $x \rightarrow 0$. This limit, however, is due to Theorem 3 not relevant for our problem since it describes trajectories, running inside the focal plane M_+ , that touch S_+ after having crossed it an infinite number of times. (These two results are different from those found for an analogous problem in [16,22]; there both limits exist and are relevant for the

system behavior.)

Now it is interesting to recall the limiting behavior of $f_\tau(x)$, cf. (42), where we found that the second term diverges as $\tau \rightarrow 0$. The first term, however, stays finite, so that

$$\lim_{\tau \rightarrow 0} f_\tau(x) = \frac{s+1}{2\omega} x - \frac{1}{\omega\tau} x_{0+} . \quad (51)$$

This means that in the present limit the lines $f_\tau(x)$ tend to be parallel to the boundary between S_- and S_+ , i.e., to the straight line W of (16).

Although the behavior of the functions $z(\tau)$ and $n(\tau)$ (especially the induced pole structure of x_τ) is interesting in its own right, we are going to restrict our discussion to the physically relevant interval of τ space. Due to Theorem 2 and 3 only τ values smaller than $2\pi/\omega$ and x values smaller than zero belong to this range. So let us first find out, which one of these two restrictions is more severe. It turns out that the second condition selects the physically meaningful interval out of τ space.

THEOREM 4 The function x_τ changes its sign at some $0 < \tau_0 < \pi/\omega$ for the first time. For all τ from the interval $(0, \tau_0)$, the curve $f(\tau)$ is smooth (C^∞) and all its points are situated inside the halfplane S_- . ***

This theorem therefore states that for the interval in question all initial points of touching trajectories show x values less than zero and are entry points of the region T_0 . Meaning, the trajectories belonging to these initial points stay inside T_0 for all $t \in (0, \tau)$.

Before proving the theorem itself, we are going to show some properties of the functions $z(\tau)$ and $n(\tau)$.

LEMMA The functions $z(\tau)$ and $n(\tau)$ have their first zeros at $\tau_1 < \pi/\omega$ and at $\tau_2 < 2\pi/\omega$, respectively, where $\tau_1 < \tau_2$. ***

PROOF of the LEMMA For reasons of abbreviation we write:

$$\begin{aligned} z(\tau) &= \omega + e_1(\tau) o_1(\tau) \\ n(\tau) &= -\omega + e_2(\tau) o_2(\tau) \end{aligned} \quad (52)$$

where

$$\begin{aligned} e_1(\tau) &:= e^\tau & , \\ o_1(\tau) &:= \omega \cos \omega \tau - \sin \omega \tau & , \\ e_2(\tau) &:= e^{(\zeta+1)\tau} & , \\ o_2(\tau) &:= \omega \cos \omega \tau - (\zeta+1) \sin \omega \tau & . \end{aligned} \quad (52a)$$

The behavior of both functions for $\tau \rightarrow 0$ we already know. There $z(\tau)$ approaches the finite value 2ω , while $n(\tau)$ vanishes to second order like $-\tau^2/2 ((\zeta+1)^2 + \omega^2)\omega$, cf. (50). Thus the first nonnegative zero of $n(\tau)$ is already found. Unfortunately the other zeros of the two functions cannot be obtained analytically, so we have to estimate (giving inequalities for) them.

Let us rewrite the equations (52) to solve ($z(\tau)=0$ and $n(\tau)=0$), by shifting the constant ω term towards the right-hand side, to obtain a more intuitive formulation of the equations:

and

$$\begin{aligned} e_z(\tau) \cdot o_z(\tau) &= -\omega \\ e_n(\tau) \cdot o_n(\tau) &= \omega \end{aligned} \tag{53}$$

Since the amplitudes of the oscillatory terms are growing exponentially, for $\tau \rightarrow \infty$ we know that the solutions of (53) converge towards the solutions of the equations

and

$$\begin{aligned} o_z(\tau) &= 0 \\ o_n(\tau) &= 0 \end{aligned} \tag{54}$$

These equations can be solved analytically and yield the results:

as well as

$$\begin{aligned} \tau_{z_n} &= \frac{1}{\omega} (\arctan \omega + n\pi) \quad , \quad n=0,1,2,\dots \\ \tau_{n_z} &= \frac{1}{\omega} (\arctan \frac{\omega}{\xi+1} + n\pi) \quad , \quad n=0,1,2,\dots \end{aligned} \tag{55}$$

Note that at these values of τ the products $e_z(\tau)o_z(\tau)$ and $e_n(\tau)o_n(\tau)$, respectively, too vanish. Although we are interested in the first positive zeros of the functions $z(\tau)$ and $n(\tau)$, i.e., in the behavior for small values of τ , the above results will help us to estimate these solutions of (53).

First let us show the existence of solutions of (53) inside the intervals $(0, \pi/\omega)$ and $(0, 2\pi/\omega)$, respectively. We just have to calculate the oscillatory terms at $\tau = \pi/\omega$ and $\tau = 2\pi/\omega$. There we find

$$o_+(0) = \omega \quad , \quad o_+(\frac{\pi}{\omega}) = -\omega$$

and

$$o_+(\frac{\pi}{\omega}) = -\omega \quad , \quad o_+(\frac{2\pi}{\omega}) = \omega \quad ,$$

since at these points the two amplitude functions $e_+(\tau)$ and $e_-(\tau)$ both show values greater than 1, we can estimate the functions $z(\tau)$ and $n(\tau)$, so:

$$z(0) = 2\omega > 0 \quad \text{and} \quad z(\frac{\pi}{\omega}) = -\omega(e^{\pi\omega} - 1) < 0$$

as well as

(57)

$$n(0) = 0, \quad n(\frac{\pi}{\omega}) = -\omega(e^{\pi\omega} + 1) < 0, \quad \text{and} \quad n(\frac{2\pi}{\omega}) = \omega(e^{2\pi\omega} - 1) > 0 \quad .$$

Hence the intermediate value theorem applies, proving the existence of solutions of (53) that are smaller than π/ω and $2\pi/\omega$, respectively.

To obtain a better estimate for the solutions of (53), let us have a look at the extremal values of $o_+(\tau)$ and $o_-(\tau)$. They are found to be situated at

$$\tau_{n\pm} = \frac{1}{\omega} (\pi - \arctan \frac{1}{\omega} + n\pi) \quad , \quad n=0,1,2 \dots$$

and

$$\tau_{\infty} = \frac{1}{\omega} (\pi - \arctan \frac{\xi+1}{\omega} + n\pi) , n=0,1,2 \dots \quad (58)$$

The mentioned extremal values, of course, are shifted by a distance of $\pi/2\omega$ from their corresponding zeros of $o_+(\tau)$ and $o_-(\tau)$, respectively. Since at these points the absolute values of both products $e_+(\tau)o_+(\tau)$ and $e_-(\tau)o_-(\tau)$ are greater than ω , we can again employ the intermediate value theorem and obtain (by looking at the first minimum of $z(\tau)$ and the first maximum of $n(\tau)$) the intervals where the solutions of (53) reside:

$$\tau_+ \in (\frac{1}{\omega} \arctan \omega, \frac{1}{\omega} (\arctan \omega + \frac{\pi}{2}))$$

and

$$\tau_- \in (\frac{1}{\omega} (\pi + \arctan \frac{\omega}{\xi+1}), \frac{1}{\omega} (\frac{3\pi}{2} + \arctan \frac{\omega}{\xi+1})) \quad (59)$$

Since for finite positive values of ξ and ω the arctan function always yields results from $(0, \pi/2)$, the intersection of the two intervals in (59) is empty and hence $\tau_+ > \tau_-$. Q.E.D.

Using the result of the Lemma, we now can give a

PROOF of THEOREM 4

Let us first look at the limiting behavior of $f_\tau(x_\tau)$ as τ approaches zero. Inserting the expression for the limiting behavior of x_τ (48,50) into equation (42) yields in this limit:

$$\lim_{\tau \rightarrow 0} f_\tau(x_\tau) = \lim_{\tau \rightarrow 0} - \left[\frac{2(\xi+1)}{\tau^2 \omega ((\xi+1)^2 + \omega^2)} + \frac{1}{\omega \tau} \right] x_{\infty} \quad (60)$$

Hence $f_1(x_\tau)$ diverges towards $-\infty$ as τ goes to zero. This yields one end of the limiting behavior of the boundary curve $\Gamma(\tau)$.

Since there is no zero of $n(\tau)$ and no zero of $\sin \omega \tau$ inside the open interval $(0, \tau_2)$ ($\tau_2 < \pi/\omega$), the functions x_τ (46) and $f_\tau(x_\tau)$ (42) show no singularities on this interval and are both smooth (in fact are C^∞).

In addition, due to the Lemma, there can be no change of sign of the function x_τ prior to τ_2 , so at $\tau = \tau_2$ the curve $\Gamma(\tau)$ leaves the halfplane $x < 0$ for the first time, selecting the physically meaningful branch of the curve, called $\Gamma_-(\tau)$.

Remains to show that this branch of the curve is situated inside S_1^+ , i.e., that for all positive values of τ smaller than τ_2 the curve $\Gamma(\tau)$ is situated to the left of the straight line W and hence the following condition

or equivalently

$$\begin{aligned} f_\tau(x_\tau) &< f_w(x_\tau) \\ f_\tau(x_\tau) - f_w(x_\tau) &< 0 \end{aligned} \tag{61}$$

is fulfilled. Inserting the results obtained so far (14b, 42, and 48) and using the identity $x_{00} = \delta$ the left-hand side of (61) may be written as:

$$F(\tau) := [f_1(\tau) - f_2(\tau) - f_3(\tau)] x_{00} \tag{62}$$

$$= \left[\left(\frac{e^{(\xi+1)\tau} - \cos \omega \tau}{2 \sin \omega \tau} - \frac{\xi+1}{2\omega} \right) \frac{z(\tau)}{n(\tau)} - \frac{e^{\tau} + \cos \omega \tau}{2 \sin \omega \tau} - \frac{1}{2\omega} \right] x_{0+} .$$

The second and third term ($f_2(\tau)$ and $f_3(\tau)$) of $F(\tau)$ are certainly positive for the interval in question and hence will yield a negative contribution, while the influence of the first term $f_1(\tau)$ is still unknown. For this function we define:

$$f(\tau) := \omega e^{(\xi+1)\tau} - \omega \cos \omega \tau - (\xi+1) \sin \omega \tau \quad (63)$$

And so $f_1(\tau)$, the first term of $F(\tau)$, can be written as:

$$f_1(\tau) = \frac{f(\tau)}{2\omega \sin \omega \tau} \frac{z(\tau)}{n(\tau)} . \quad (64)$$

About the second factor ($z(\tau)/n(\tau)$) we already know that it is negative for the interval $(0, \tau_0)$ in question, while the sine function in the denominator of the first factor is certainly positive there, so let us investigate the behavior of $f(\tau)$. Here we find at the origin

$$\begin{aligned} f(0) &= 0 , \\ f'(0) &= 0 , \\ f''(0) &= \omega((\xi+1)^2 + \omega^2) , \end{aligned} \quad (65)$$

with " ' " meaning the derivative with respect to τ .

This shows that $f(\tau)$ possesses a minimum at the origin. Here again we can apply the Lemma from the Appendix (after a

shifting of the phase and a rescaling of the amplitudes) finding that all subsequent minima of $f(\tau)$ take values greater than zero. Hence $f(\tau)$ shows positive values for all $\tau > 0$, it especially does not change its sign inside the open interval $(0, \tau_1)$.

So far we have demonstrated that the three terms of the function $F(\tau)$ all separately yield negative contributions for the range of τ mentioned. This means that the whole function only takes negative values inside the interval $(0, \tau_1)$, and hence $\Gamma(\tau)$ is situated completely inside the interior of S_1^* . Q.E.D.

Note that in the function $f_1(\tau)$ for $\tau \rightarrow 0$ the factors $f(\tau)$ and $n(\tau)$ cancel (except for the sign) and hence the first and second term of $F(\tau)$ both diverge only to first order like $-1/\omega\tau$ (independently of the canonical parameter ξ), yielding in this limit:

$$\lim_{\tau \rightarrow 0} F(\tau) = -\left[\frac{2}{\omega\tau} + \frac{1}{2\omega}\right] x_{0*} \quad (66)$$

3.5. Conclusion

By now, the domains of the transfer and return maps inside the halfplane S_1^* have been demonstrated explicitly by calculating their boundaries. Thus we know that the halfplane of entry points is divided into three portions: (1) $\mathcal{D}(\mathcal{T})$ the domain of the transfer map \mathcal{T} containing all points with x values

greater than zero as well as the points of Σ_+ to the left of ξ_0 and the points of S_+ to the left of the curve $\Gamma_+(\tau)$; i.e., those entry points of T_+ with absolute values of ξ , and hence initial radius, big enough. (2) $\mathcal{D}(\mathcal{R})$ the domain of the return map \mathcal{R} containing the points with negative values of x in between the curve $\Gamma_+(\tau)$ and the straight line W_+ . (3) The basin of attraction of the saddle-focus L_+ (which, due to the saddle character of the steady state, is just the ξ interval $(\xi_0, \delta/2\omega)$ on the straight line Σ_+ , so that it is of measure zero inside the plane S_+).

Fig. 9

Note that $\xi_{T_2}(x_{T_2})$, the ξ value of the end point of $\Gamma_+(\tau)$, is equal to ξ_0 , the end point of the basin of attraction of the steady state L_+ . Thus it suffices to determine either ξ_0 - by the mentioned fixed point algorithm, for example - or T_2 , using a root finder, like Newton's method, for example.

In practice $\xi_0 = \xi_{T_2}(x_{T_2})$ can be calculated from T_2 , but on the other hand T_2 cannot be found analytically from ξ_0 . So the second way yields the result faster. However, computing both quantities independently gives a good criterion for the consistency of the calculations.

4. Criteria for the Appearance of the Double-Scroll Attractor

After having characterized the behavior of the system inside the intermediate state space region T_+ , let us finally discuss some

criteria for the appearance of the double-scroll attractor. Due to the symmetry of the problem it suffices to treat just one half of the state space; let us choose the one with u values less than zero.

The attractor itself is well characterized in [5], so we omit this task here. We just mention one fact: The two steady states L_+ and L_- , like L_0 , are of the saddle-focus type. The character of the dynamics acting inside T_+ (and inside T_- as well), however, is of the opposite type to the dynamics of T_0 , i.e., the real eigenvalue turns out to be negative while the real part of the two complex conjugate eigenvalues is greater than zero.

The first criterion for the appearance of the double-scroll, as already mentioned above, is the reality of the steady state L_+ (and, equivalently L_-), i.e., $k > \delta$ (cf. (4a)). Otherwise, if this steady state would be a virtual one, the only possible type of intersection curves of the dynamical manifolds from T_+ with the separating plane S_+ would be Ω -curves. Hence every trajectory entering T_+ would leave this region after more or less half a turn around the real eigenvector [13] of L_+ and thus no scroll structure could be found inside this region.

Let us now apply the results of [13] to the dynamics acting on T_+ . For the appearance of a scroll structure inside this region of state space a trajectory has to run several times around

the unstable manifold (real eigenvector) of the steady state L , i.e., its entry point must be situated either on a simple isola corresponding to the dynamics of T , or on that portion of a complicated isola that is not mapped to the other part of the same isola, situated inside the range of the halfmap. In consequence the corresponding exit point is situated on the base line belonging to the isola in question.

If the relaxation towards the focal plane of the steady state is fast enough, as is the case in the example treated in [5], where $\xi = 20.74$ was found (note that since we discuss different dynamics in the present Section, we add an index "-", "0", or "+", respectively, to the quantities characterizing the dynamics), all base lines are located very close to the intersection line of the focal plane of L with S , called Σ_- (this is not to be confused with the Σ_0 belonging to the dynamics of T_0). For this example the base lines are almost indistinguishable from this intersection line (see Fig. 10). To give a rough estimate of this fact we calculate the Cartesian point x_- [13] that is the limit of all maximum distances of the base lines from the line Σ_- . This quantity turns out to be $(\delta - k) / (\xi + 1) = 0.046(\delta - k)$, i.e., less than 5% of the distance that the intersection point of the real eigenvector has from Σ_- .

Fig. 10

So we can treat the question of exit points (with the corresponding entry points being situated on an isola) as an almost "flat spiral problem" [16] and calculate the interval of possible exit points along Σ_- (in close analogy to what we did

for Σ_{\bullet} , calculating the basin of attraction of the steady state L_{\bullet}). Now it is not hard to find out whether this portion of Σ_{\bullet} intersects (in a set theoretical sense) both the domains of the transfer and the return map, or whether it intersects just one of them (cf. Fig. 10). This yields a sufficient condition for the appearance of transferring trajectories inside a chaotic attractor. If, on the other hand, the mentioned portion of Σ_{\bullet} does not intersect the domain of \mathcal{T} , there may, nevertheless, exist entry points of T_{\bullet} , situated on Ω -curves of T_{\bullet} that lead to transferring trajectories of a chaotic attractor.

For the case of a slow relaxation towards the focal plane inside the region T_{\bullet} , the "flat spiral exit points" are a poor approximation of the real system behavior and hence one has to investigate the intersection of the image of all isolae with the domains of the maps \mathcal{T} and \mathcal{R} , respectively. This needs a little more effort. It can be done, however, by calculating the Cartesian leaf, as a limiting case for isolae, with all its boundaries inside S_{\bullet}^* . (This is shown in [22].) Thereafter one has to take the intersection with the domains of the two point transformations, acting on T_{\bullet} .

As a last step let us, for a moment, think of the dynamics of T_{\bullet} , and hence the structures determined by this dynamics, as fixed. Then by varying S_{\bullet} and ω_{\bullet} (the canonical parameters of the dynamics of T_{\bullet}) we can change the domains of the transfer and return map to intersect the relevant exit points of T_{\bullet} .

(or not to do so, respectively). Calculating the limiting conditions for such intersections yields relations between S_0 and ω_0 . These relations lead to a charting of the canonical parameter space of the dynamics of T_0 , similar to the charts presented in [13,22]. A detailed discussion of this topic, however, will be the subject of a subsequent paper [23].

5. Discussion

In this paper we treated a piecewise-linear continuous dynamical system showing the "piecewise-linear double-scroll" [5] (for a topological equivalent nonlinear system cf. [24]) and other types of chaotic attractors [17]. The special appeal of this model is its being realized in Chua's circuit [5] and hence an experimentally easy to handle real life system (behaving almost piecewise-linearly). Our aim was to obtain a better understanding of the appearance of chaotic solutions of this system by means of dynamical structures present inside the intermediate region of state space. (The contributions to the chaotic behavior coming from the dynamics of the regions T_1 and T_2 , respectively, can be described by means of Poincaré halfmaps [22].)

The system in question is among the simplest of the piecewise-linear type. The switching of dynamics is controlled by just one variable (u), and hence the boundaries of the different regions of state space are two parallel, flat (so called

separating) planes. In addition, the equation of motion is antisymmetric, so all statical and dynamical structures of the state space, including the attractors, have to possess the same symmetry. This means that the mentioned structures either themselves are antisymmetric with respect to the origin or appear twice, like a pair of particle and antiparticle.

Nevertheless, as there are more than two regions present in state space, new problems, not treated in the literature until now, arise. In the present case two different kinds of regions have to be distinguished. The first type, the leftmost and rightmost regions, T_1 and T_2 , respectively, is well known from the theory of Poincaré halfmaps: it is limited by one boundary only and hence the whole dynamics inside can be characterized by the intersection of its dynamical manifolds with the single separating plane present as was found. For the other type, the intermediate region, two boundaries exist, giving this region a finite extension in one direction of state space. Here too, the dynamics is described completely by the intersection curves of the dynamical manifolds with the separating planes. These intersection curves, however, are only partially physically meaningful (and partially not). This is due to the fact that two switching conditions are competing for the smallest solution, i.e., the first time that the trajectory in question leaves the region.

The two generic types of behavior inside the intermediate region give rise to two different point transformations, which

were called transfer and return maps, respectively. For the example of the double-scroll attractor both maps are made use of by a solution running inside the attractor. So, in addition to the separating mechanisms that stem from the dynamics of the leftmost and rightmost regions T_1 and T_2 , respectively [22], another separating and hence potentially chaos producing structure appears for the intermediate region T_0 . Two trajectories having adjacent entry points into T_0 and being situated on both sides of the curve $\Gamma_0(\tau)$ (i.e., inside the domains of different maps) are separated very fast. While one solution returns to the region it came from, the other transfers the intermediate region and eventually enters the third region of state space. So after an interval of time of about $2\pi/\omega$, two adjacent points are found at opposite ends of the attractor. This is an excellent example for a "sensitive dependence on initial conditions" [25]. If this mechanism is used by the trajectories running inside the attractor, it readily gives rise to a positive Lyapunov exponent [26].

The boundary between the domains of the two point transformations in question can be determined by picking up the initial points of touching trajectories. These special orbits, in the case treated, enter the region T_0 through one separating plane, say S_1 , and after about half a turn around the stable manifold of the steady state fulfill the other switching condition at their maximum u values, i.e., at points of the straight line W_1 , thus being transversal points. This means that trajectories with the same initial x value as a touching

trajectory and closely adjacent ξ values will either leave the region T_0 close to the touching point or stay inside this region temporarily in order then eventually to leave T_0 towards T_1 again.

Although the farmost biggest portion of the separating plane S_0 is covered by $\mathcal{D}(\mathcal{T})$, the domain of the transfer map \mathcal{T} , for the present system also attractors were found without any transferring solutions, cf. [17]. These solutions can in fact be described by means of even simpler, two region, models. In this case the separatrix in between the two symmetric attractors is exactly of dimension two and can be calculated explicitly [27]. On the other hand it is also not hard to construct a system without returning trajectories inside the attractor. The crucial point is the matching of the different dynamics. There is just one severe restriction on the interaction of the dynamics that is due to the C^1 character of the flow, (leaving the two lines W_0 invariant for the different dynamics), while the intersections of the statical manifolds of the dynamics with the separating planes are almost completely arbitrary. So by shifting these structures relatively to each other, the character of the attractor, if there is any at all present, can be determined.

To conclude, the results presented here concerning the properties of the transfer and return maps are completely independent of the special example system and the parameters chosen. They are valid for all piecewise-linear dynamical systems possessing intermediate regions with a steady state of saddle-focus

November 29, 1985

type and the discussed symmetry properties. Thus our results provide an universal tool for the treatment of a whole class of dynamical systems.

Appendix

Here we show some properties of functions that are the sum of an exponential and an oscillatory term. This kind of functions appears several times in this paper (20, 47, and 63).

LEMMA from Analysis For positive values of its argument, the function

$$F(t) = e^t + a \sin \omega t \quad (\text{A.1})$$

possesses either no or a finite even number of zeros and extrema (counted including degeneracies). The phase shift of subsequent zeros or extrema, respectively, grows monotonically in absolute value. ***

PROOF We assume $a > 0$ and $\omega > 0$; the case $a < 0$ can be treated similarly by shifting the phase by $-\pi$ and rescaling the amplitude with $e^{\pi/\omega}$; for $\omega < 0$ one finds $a \sin -\omega t = -a \sin \omega t$ so that the above procedure goes through again.

First we show that for positive values of t there is at most a finite number of disjoint intervals of length $2\pi/\omega$ that contain zeros of $F(t)$. At $t = t_{\max} := \ln a$, the exponential reaches the value of the amplitude a of the sine and hence there can be no zero of $F(t)$ for values greater than t_{\max} . So all roots of $F(t)$ are situated inside the interval $(0, \ln a]$. Since a is finite this interval can be covered completely by a finite

union of disjoint intervals of length $2\pi/\omega$.

In the following it suffices to look at the interval $(0, 2\pi/\omega]$. All the subsequent intervals of this length can be treated by shifting t for $2\pi/\omega$ and rescaling the amplitude a by a factor of $e^{-2R\omega}$.

For $0 < t < \pi/\omega$ both terms of $F(t)$ are positive so there can be no zero inside this interval. Hence a first negative criterion for the existence of a zero of $F(t)$ is

$$t_{\text{max}} \leq \frac{\pi}{\omega}, \quad a \leq e^{\pi/\omega} \quad (\text{A.2})$$

In this case, no zero can occur since for all subsequent values of t the maximal absolute value of the sine cannot compensate for the exponential. On the other hand a positive criterion would be:

$$t_{\text{max}} \geq \frac{3\pi}{2\omega}, \quad a \geq e^{3\pi/2\omega}, \quad (\text{A.3})$$

Here, the intermediate value theorem assures a zero inside the interval $(\pi/\omega, 3\pi/2\omega]$ since

$$F\left(\frac{\pi}{\omega}\right) = e^{\pi/\omega} > 0$$

and

$$F\left(\frac{3\pi}{2\omega}\right) = e^{3\pi/2\omega} - a \leq 0 \quad (\text{A.4})$$

For $t_{\text{zer}} \in (\pi/\omega, 3\pi/2\omega)$, no criterion exists. However, if there is a zero of $F(t)$ present, it must be situated inside $(\pi/\omega, t_{\text{zer}})$.

The possible orders of the zeros of $F(t)$ are easily found by looking at a power series expansion of this function at a zero. Let us assume a zero at $t=t_1$; then (as all functions that appear are analytical)

$$\begin{aligned} F(t) &= F(t_1) + F'(t_1)(t-t_1) + \frac{1}{2}F''(t_1)(t-t_1)^2 + \dots \\ &= (e^{t_1} + a \sin \omega t_1) + (e^{t_1} + a\omega \cos \omega t_1)(t-t_1) \quad (\text{A.5}) \\ &\quad + \frac{1}{2}(e^{t_1} - a\omega^2 \sin \omega t_1)(t-t_1)^2 + \dots \end{aligned}$$

By construction the first term vanishes ($F(t_1)=0$), implying:

$$e^{t_1} = -a \sin \omega t_1 \quad (\text{A.5a})$$

If the zero is of order two, the second term too must be equal to zero. As a criterion for this type of zero we obtain

$$t_1 = \frac{1}{\omega} \arctan \omega \quad (\text{A.5b})$$

For the third term we find, using the above results:

$$\begin{aligned} F''(t_1) &= -a(1+\omega^2) \sin \omega t_1, \\ &= -a\sqrt{1+\omega^2} \neq 0 \quad (\text{A.5c}) \end{aligned}$$

As this term cannot vanish unless $a=0$, the highest possible order of zeros that may appear in $F(t)$ is two.

To see that the roots of $F(t)$ always appear in pairs we again employ the intermediate value theorem. First of all we find that $F(\pi/\omega) = e^{\pi/\omega} > 0$. Let the first zero of $F(t)$ be situated at $\pi/\omega < t_1 < 3\pi/2\omega$, and let us, for a moment, assume this zero to be of first order. Then $F'(t_1) < 0$, meaning that there is an open interval (t_1, t'_1) with $F(t) < 0$ for all values of t belonging to this interval. For $t = 2\pi/\omega$, however, we know $F(2\pi/\omega) = e^{2\pi/\omega} > 0$, so the intermediate value theorem guarantees the existence of another first order zero at t_2 , present in the interval $(t'_1, 2\pi/\omega)$. Since $F'(t_2) > 0$, this is the last zero in this interval.

Now it is easy to see also that there is no other zero present inside (t_1, t_2) . We just have to investigate the behavior of the derivative of $F(t)$. For $\pi/\omega < t < 2\pi/\omega$ and hence for $t \in (t_1, t_2)$, the derivatives of both the sine and the exponential are strictly increasing, so the curvature of $F(t)$ is always positive for this region. This excludes another pair of zeros inside the interval in question.

Let us now estimate the deviation of the zeros of $F(t)$ from the corresponding zeros of the pure sine function. To this end we write the equation $F(t) = 0$ as

$$t = \frac{1}{\omega} \arcsin\left(-\frac{e^t}{a}\right) . \quad (A.6)$$

This shows that when picking the pertinent branch of the arcsine function, the zeros of $F(t)$ showing negative slope will appear retarded (and those with positive slope advanced) compared to the zeros of the pure sine function. In either case the absolute value of the argument of the arcsine for subsequent zeros of $F(t)$ increases and so does, due to the monotone behavior of the arcsine, the absolute value of the deviation (phase shift).

This shows that only the last zero of $F(t)$ can be of second order. In this case the sum of the absolute values of the shifts corresponding to t_1 and t_2 yields exactly π/ω . So the two first order zeros coalesce. This can only happen inside the interval $(\pi/\omega, 3\pi/2\omega)$, yielding $t_{\text{max}} < 3\pi/2\omega$, and hence there are no further zeros present

The behavior of the derivative of $F(t)$ can be investigated in a completely analogous fashion. Here we have to treat the function

$$F'(t) = e^t + a\omega \cos \omega t . \quad (A.7)$$

It can be brought into the form of (A.1) by introducing a new amplitude $a' := \omega a$ and shifting the t axis by an amount of $-\pi/2\omega$ (i.e., rescaling the amplitude by a factor of $e^{\pi/2\omega}$ and

November 29, 1985

converting the cosine into a sine). This procedure neither adds nor removes any zero of the function. Thereafter all arguments carry through unchanged. **Q.E.D.**

Acknowledgment

This work was supported by the DFG.

References

- [1] O.E. Rössler, The gluing-together principle and chaos, in Nonlinear Problems of Analysis in Geometry and Mechanics, M. Atteia, D. Bancel, and I. Gumowski, Editors, Pitman, Boston, 1981, pp. 50-56.

- [2] C.T. Sparrow, Chaos in a three dimensional single loop feedback system with a piecewise linear feedback function, J. Math. Anal. Appl., 83 (1981), pp. 275-291.

- [3] B. Uehleke and O.E. Rössler, Complicated Poincaré half-maps in a linear system, Z. Naturforsch., 38a (1983), pp. 1107-1113.

- [4] C. Kahlert and O.E. Rössler, Chaos as a limit in a boundary value problem, Z. Naturforsch., 39a (1984), pp. 1200-1203.

- [5] T. Matsumoto, L.O. Chua and M. Komuro, A chaotic attractor from Chua's circuit, IEEE Trans. Circuits Syst., Vol.CAS-32, pp. 797-818, August, 1985.

- [6] R.W. Rollins and E.R. Hunt, Exactly solvable model of a physical system exhibiting universal chaotic behavior, Phys. Rev. Lett., 49 (1982), pp. 1295-1298.

- [7] J.N. Schulman, Chaos in piecewise-linear systems, Phys. Rev. A, 28 (1983), pp. 477-479.

- [8] T. Matsumoto, L.O. Chua, and S. Tanaka, Simplest chaotic nonautonomous circuit, Phys. Rev. A, 30 (1984), pp. 1155-1157.

- [9] L. Danziger and G.L. Elmergreen, The thyroid-pituitary homeostatic mechanism, Bull. Math. Biol., 18 (1956), pp. 1-13.

- [10] J. Rinzel and J.B. Keller, Traveling wave solutions of a nerve conduction equation, Biophys. J., 13 (1973), pp. 1313-1337.

- [11] J.M.T. Thompson, Complex dynamics of compliant off-shore structures, Proc. R. Soc. Lond., A387 (1983), pp. 407-427.

- [12] G.-Q. Zhong and F. Ayrom, Experimental confirmation of chaos from Chua's circuit, Int. J. Circuit Theory and Applications, 13 (1985), pp. 93-98.

- [13] C. Kahlert and O.E. Rössler, Analytical properties of Poincaré halfmaps in a class of piecewise-linear dynamical systems, Z. Naturforsch., 40a (1985), pp. 1011-1025.

- [14] C. Kahlert, Existence and uniqueness of solutions of piecewise-defined dynamical systems, submitted to Z.

Naturforsch., 1985.

- [15] N. Minorsky, *Nonlinear Oscillations*, Robert E. Krieger Publishing Company, Huntington, 1974.

- [16] C. Kahlert, *Infinite Nonperiodic Wavetrains in a Class of Reaction-Diffusion-Equations - Analytical Properties of Poincaré Halfmaps (in German)*, Ph.D. Thesis, University of Tübingen, 1984.

- [17] T. Matsumoto, L.O. Chua and M. Komuro, *Bifurcation phenomena in a third order electrical circuit*, preprint 1985.

- [18] F. Ayrom, *personal communication*, 1985.

- [19] L.O. Chua and R.L.P. Ying, *Canonical piecewise-linear analysis*, *IEEE Trans. Circuits Syst.*, CAS 30 (1983), pp. 125-140.

- [20] C. Kahlert and O.E. Rössler, *Finite wavetrains in a one-dimensional medium*, *Z. Naturforsch.*, 38a (1983), pp. 648-667.

- [21] M.W. Hirsch and S. Smale, *Differential Equations, Dynamical Systems, and Linear Algebra*, Academic Press, New York, 1974.

- [22] C. Kahlert, The chaos-producing mechanism in Poincaré halfmaps, in preparation.

- [23] C. Kahlert, The composition of Poincaré halfmaps and chaotic attractors, in preparation.

- [24] O.E. Rössler, Continuous Chaos, in Synergetics - A Workshop, H. Haken, Editor, Springer Verlag, Berlin, 1977, pp. 184-197.

- [25] D. Ruelle, Sensitive dependence on initial conditions and turbulent behavior of dynamical systems, in Bifurcation Theory and its Applications in Scientific Disciplines, O. Gurel and O.E. Rössler, Editors, Ann. New York Acad. of Sci., 316 (1979), pp. 408-416.

- [26] V.I. Oseledec, A multiplicative ergodic theorem. Lyapunov characteristic number for dynamical systems, Trans. Moscow Math. Soc, 19 (1968), pp. 197.

- [27] C. Kahlert, A manifold separating the basins of two chaotic attractors, in preparation.

Captions

Figure 1 Numerical integration of Equation (1) for $T = 0 \dots 250$. The trajectory shown runs inside the attractor. One sees that sometimes it changes from one scroll to the other (transferring the intermediate region bounded by the two planes S_+ and S_-) and sometimes it enters the intermediate region in order to only return towards the same scroll. System parameters: $a = 9$, $b = 14 \frac{2}{7}$, $n_0 = -5/7$, $n_1 = -8/7$, $\delta = 1$. Axes for the state space plot: $u = -2.2 \dots 2.2$, $v = -0.4 \dots 0.4$, $w = -3.25 \dots 3.25$. Axes for the time plots: $u = -2.2 \dots 2.4$, $v = -0.4 \dots 0.45$, $w = -3.25 \dots 3.5$, $T = 0 \dots 250$.

Figure 2 Geometry of the separating plane S_+ in a x, ξ representation. The sets of entry (S_+^*) and exit points (S_+^-) of the region T_0 are indicated as well as the two straight lines Z_+ (see text of next Section) and W_+ (which includes the point x_0). Parameters: $\xi = 1$, $\omega = 1$, $\delta = 1$. Axes: $x = -1 \dots 1$, $\xi = -1 \dots 1$.

Figure 3 A dynamical manifold \mathcal{M} , truncated by the two separating planes S_+ and S_- . For the example shown, the branch of \mathcal{M} having positive x values, i.e., the branch above the unstable manifold M_u , intersects S_+ in an isola plus its corresponding base line, while an Ω -curve is found for the intersection with the plane S_- . For values of x less than zero, the opposite holds true. Parameters: $\xi = 1$, $\omega = 2$, $\delta = 1$. Axes: $x = -0.25 \dots 1.25$, $\eta = -1.125 \dots 0.625$, $\xi = -1.25 \dots 1.25$. Here

and in the following figures visualizing the state space the origin is indicated by a "X" while an "O" marks the positions of the points h_2 (being the intersection points of the stable manifold M_s with the separating planes S_+ and S_- , respectively).

Figure 4 Three trajectories running inside the unstable manifold M_u . The touching trajectory is the limiting case. For absolute values of the initial ξ greater than ξ_0 , the trajectory leaves T_+ entering T_- , while for smaller absolute values of ξ the trajectory is attracted by the steady state L_+ . Note that no trajectory can return to the region T_- . Parameters: $\omega = 7.5$, $\delta = 1$, $r_1 = 1.66 (=1.1r_2)$, $r_2 = 1.51$, $r_3 = 1.36 (=0.9r_2)$.

Figure 5 Examples for a transferring and a returning trajectory with initial points being from S_- . Parameters: $\xi = 1$, $\omega = 2$, $\delta = 1$. Axes: $x = -1.25 \dots 1.25$, $\eta = -1.125 \dots 1.125$, $\xi = -0.9 \dots 0.9$. Initial coordinates for the transferring trajectory: $x_{ot} = x_{or} + 0.375$, $\xi_{ot} = \xi_{or}(x_{ot}) - 0.3$; and for the returning trajectory: $x_{or} = 0.1$, $\xi_{or} = \xi_{or}(x_{or}) - 0.5$.

Figure 6 Example of a touching trajectory also showing two other orbits starting at the same x value but having closely adjacent values of the initial ξ . Parameters: $\xi = 1$, $\omega = 2$, $\delta = 1$. Axes: $x = -1.5 \dots 1$, $\eta = -1 \dots 1.25$, $\xi = -2 \dots 1$. Initial x values for all three trajectories: $x_0 = -0.281$. For the touching, transferring, and returning trajectory, respectively, the initial ξ values are: $\xi_{or} = -1.62$, $\xi_{ot} = \xi_{or} - 0.25$, $\xi_{or} = \xi_{or} + 0.25$.

Figure 7 Schematic representation of trajectories running inside the region T_+ under the dynamics of T_+ . For $\Delta\tau \rightarrow 0$ these orbits necessarily approach a touching trajectory.

Figure 8 The lines of equal mapping duration $f_\tau(x)$ in the $x < 0$ portion of the separating plane S_- for $\tau = 0.1 \dots \pi/\omega$, with increment $\Delta\tau = 0.0236$. Since $\Delta\tau$ is rather small, the intersection points of these lines virtually coincide with entry points of touching trajectories (cf. text). Parameters: $\xi = 1$, $\omega = 1$, $\delta = 1$. Axes: $x = -2 \dots 0.2$, $f = -8 \dots 1$.

Figure 9 Partition of the separating plane S_- . The curve Γ is the geometric locus of all initial points of touching trajectories. Only the portion of this curve with x values less than zero (Γ_-) yields physically meaningful results and is plotted. Parameters: $\xi = 1$, $\omega = 1$, $\delta = 1$. Axes: $x = -2 \dots 0.2$, $f = -8 \dots 1$.

Figure 10 The plane S_- ($u = -1$) in a v, w representation (original coordinates).

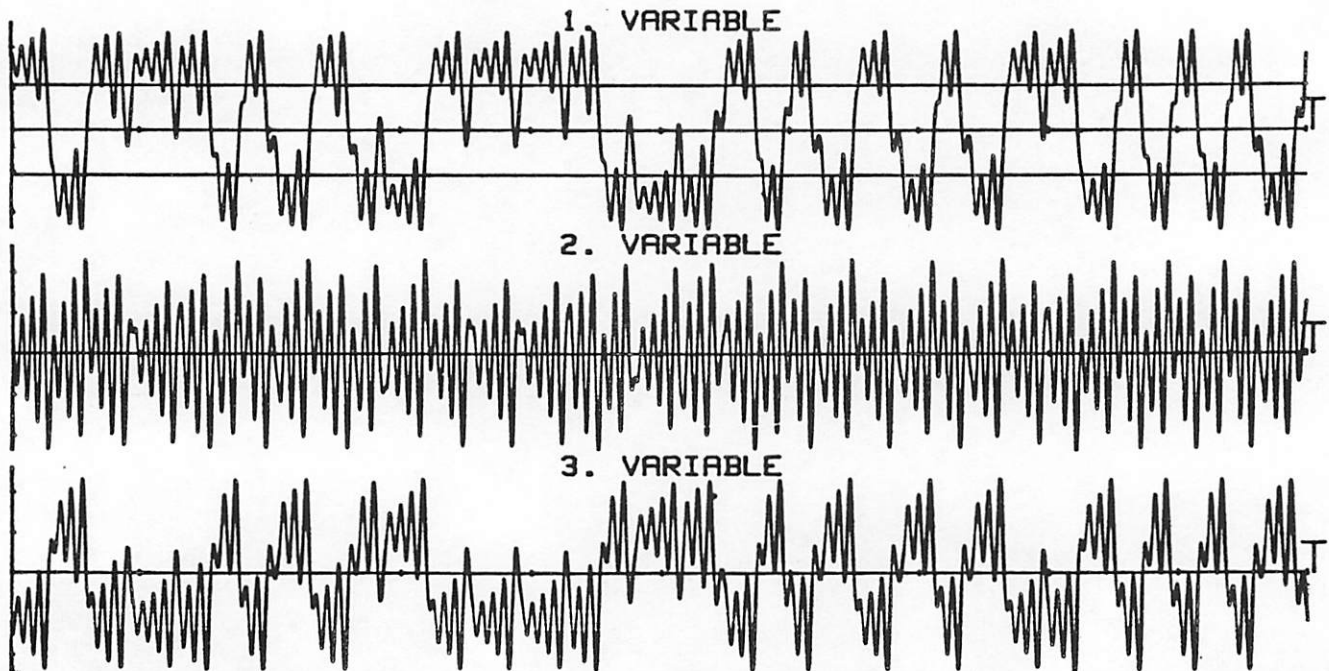
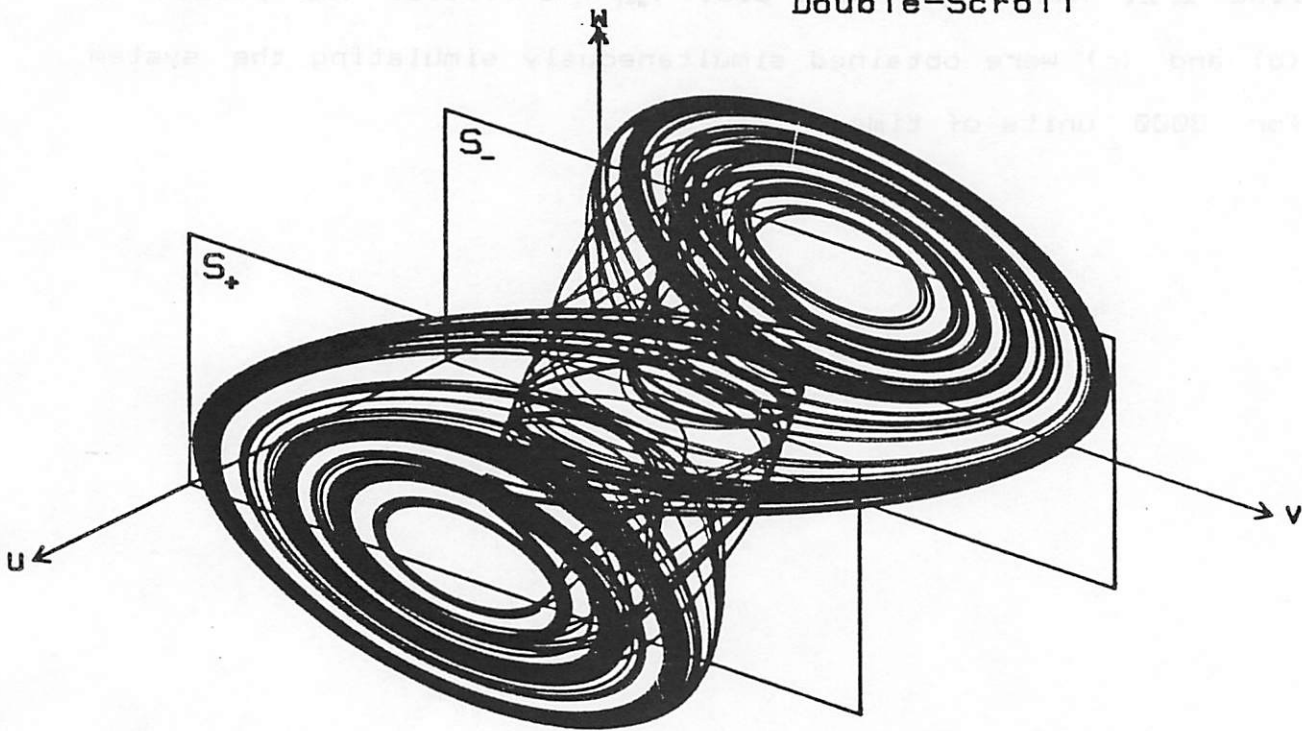
(a) The solid portions of the dashed straight lines Z_+ and Z_- are the basin of attraction of the steady state L_+ and the "flat spiral exit points" of T_+ (cf. text), respectively. For a continuation (run for 300 units of time) of the solution shown in Fig. 1 the entry points of the region T_+ are indicated by an "E" while a "X" is used for the exit points. Axes: $v = -0.3 \dots 1$, $w = 0 \dots 2.5$.

(b) Poincaré cross section showing the exit points of T_0 . Axes: $v = -0.3 \dots 0.2$, $w = 0 \dots 1.2$.

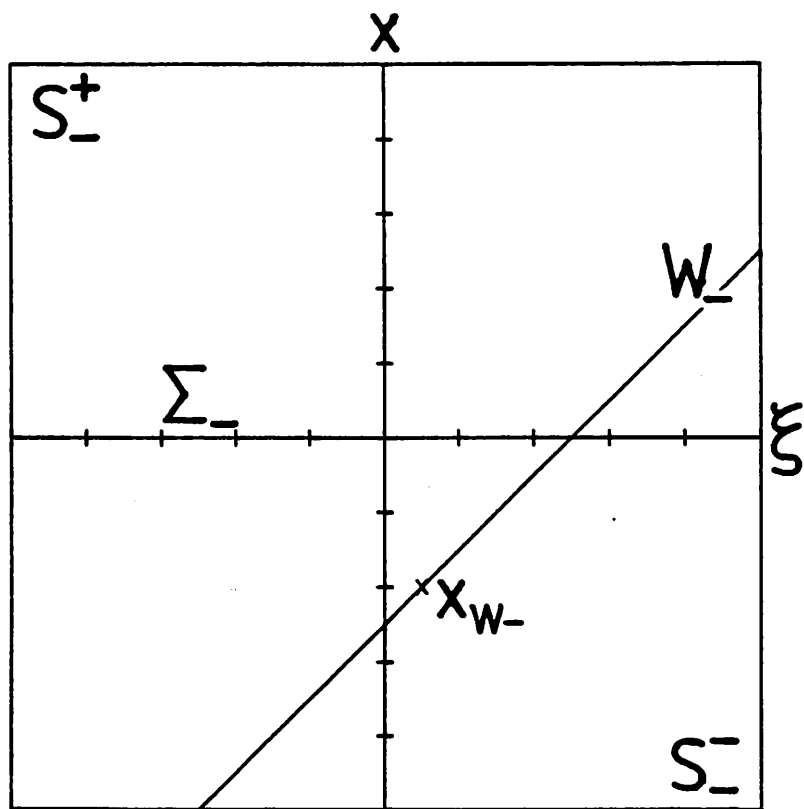
(c) One-dimensional map for the v component of the entry points of T_0 , being situated almost exactly on the straight line Σ . Axes: $v_n = -0 \dots 0.5$, $v_{n+1} = 0 \dots 0.5$. The points of (b) and (c) were obtained simultaneously simulating the system for 8000 units of time.

Fig. 1

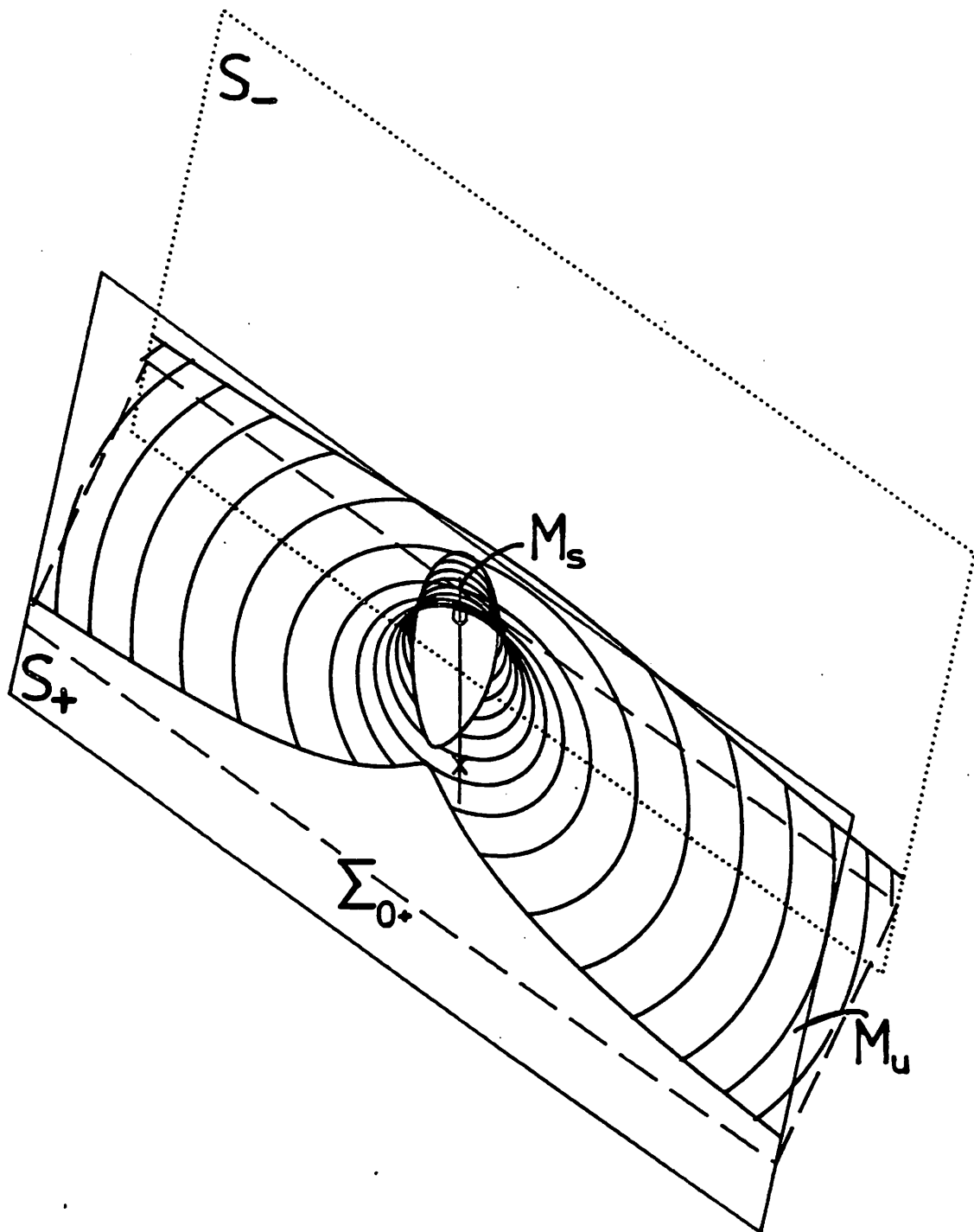
Double-Scroll



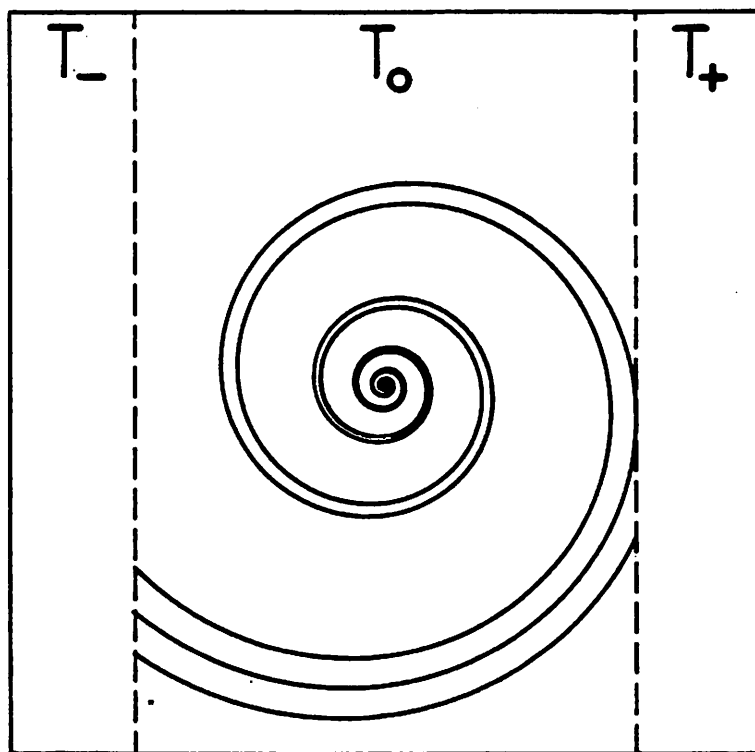
Kahler & Chua Fig. 2



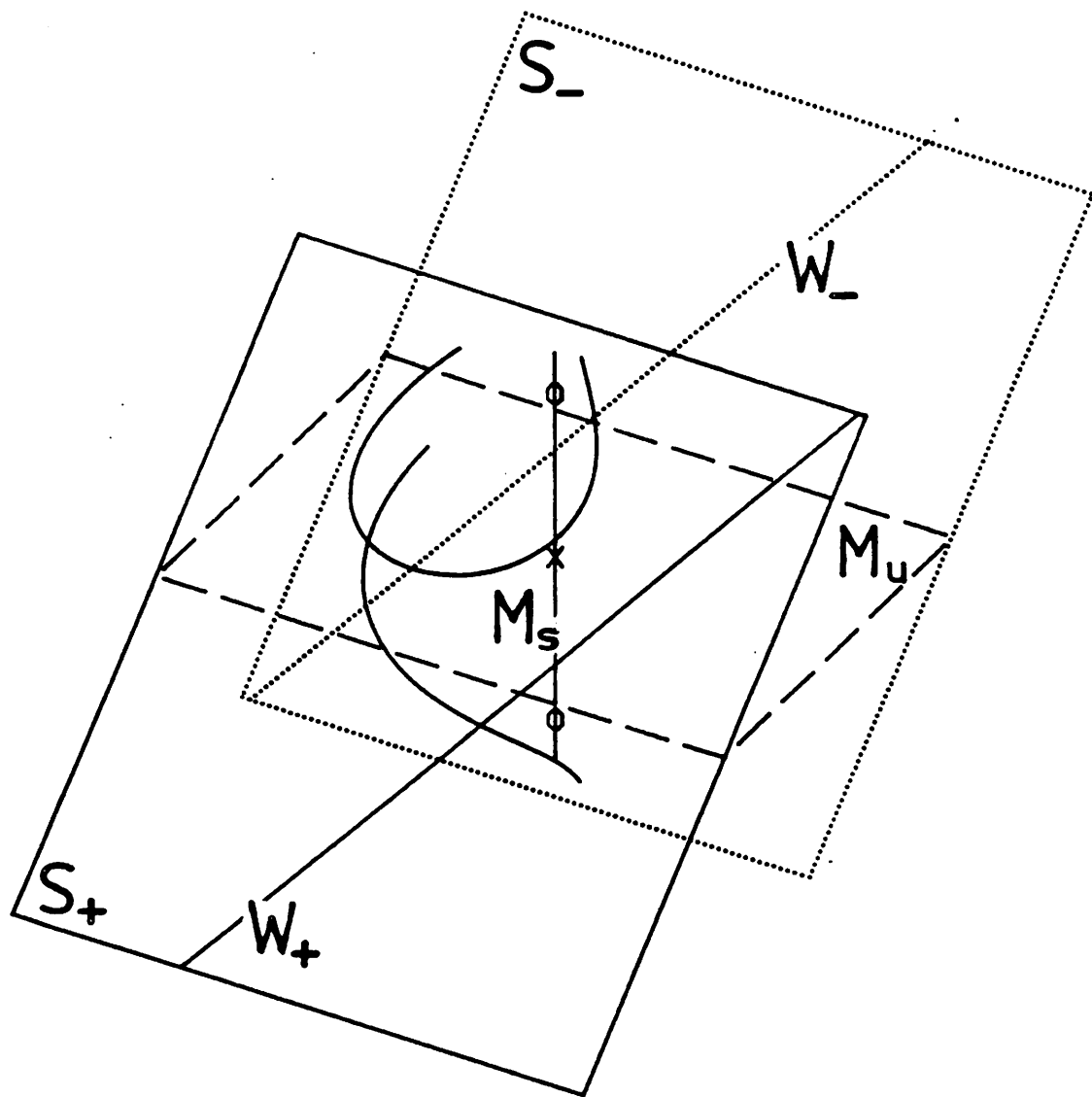
Kahler & Chua Fig. 3



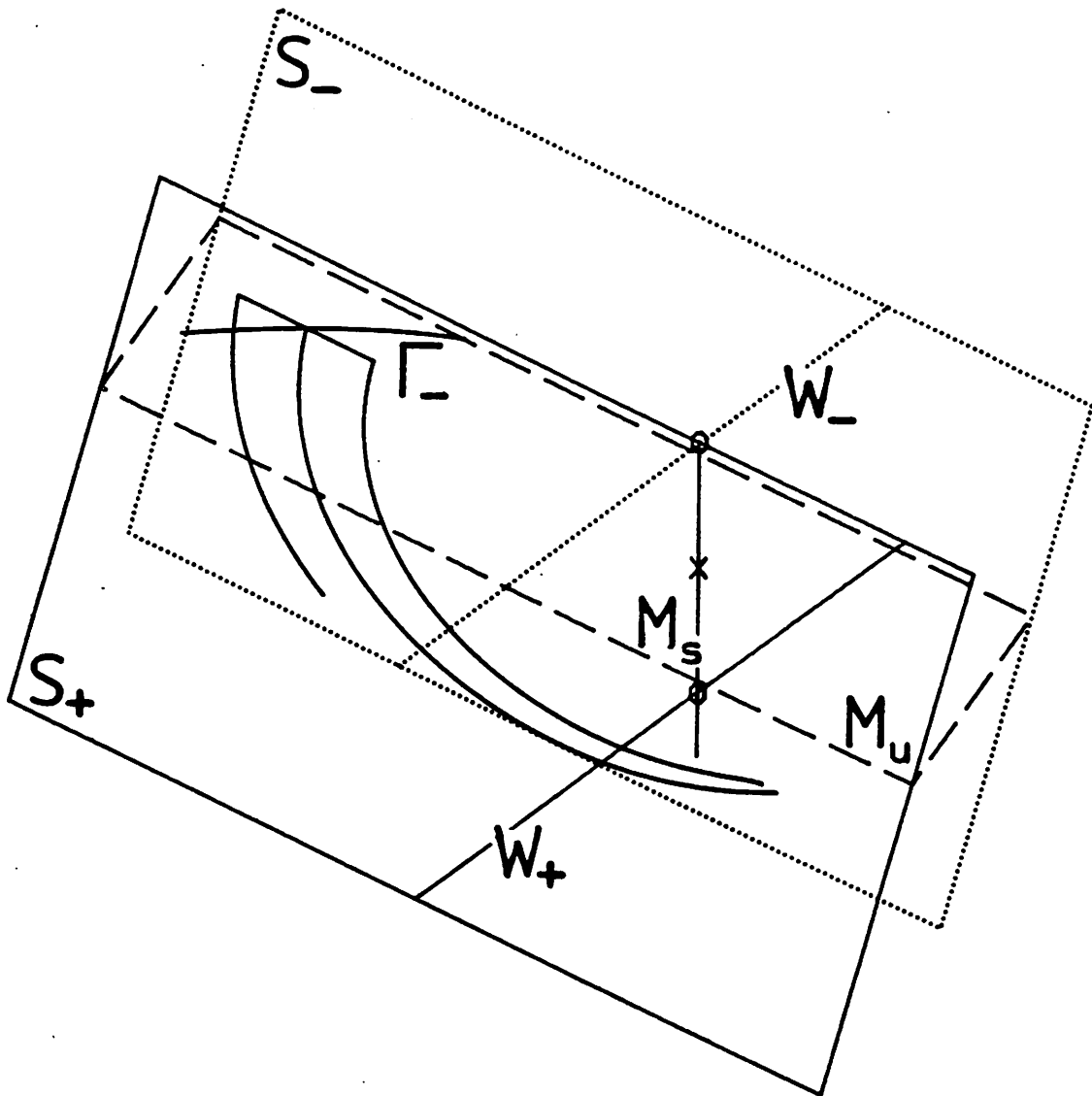
Kahlert & Chua Fig. 4



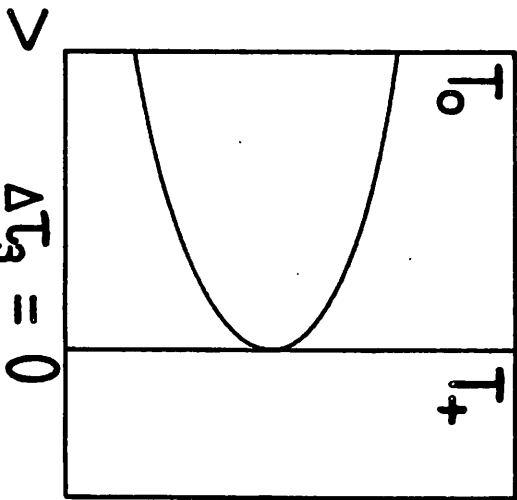
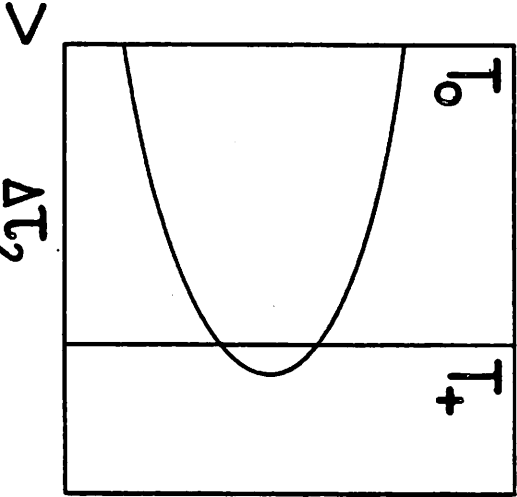
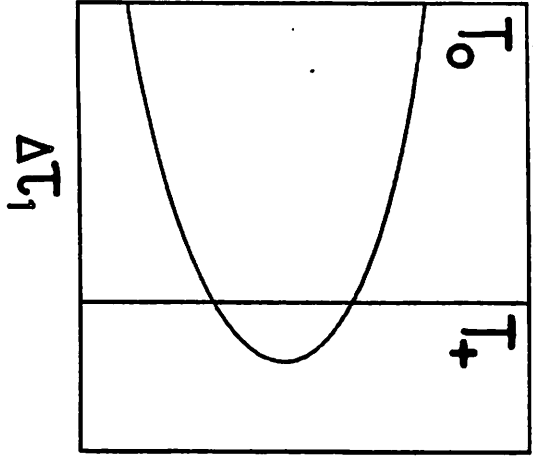
Kahlert & Chua Fig. 5



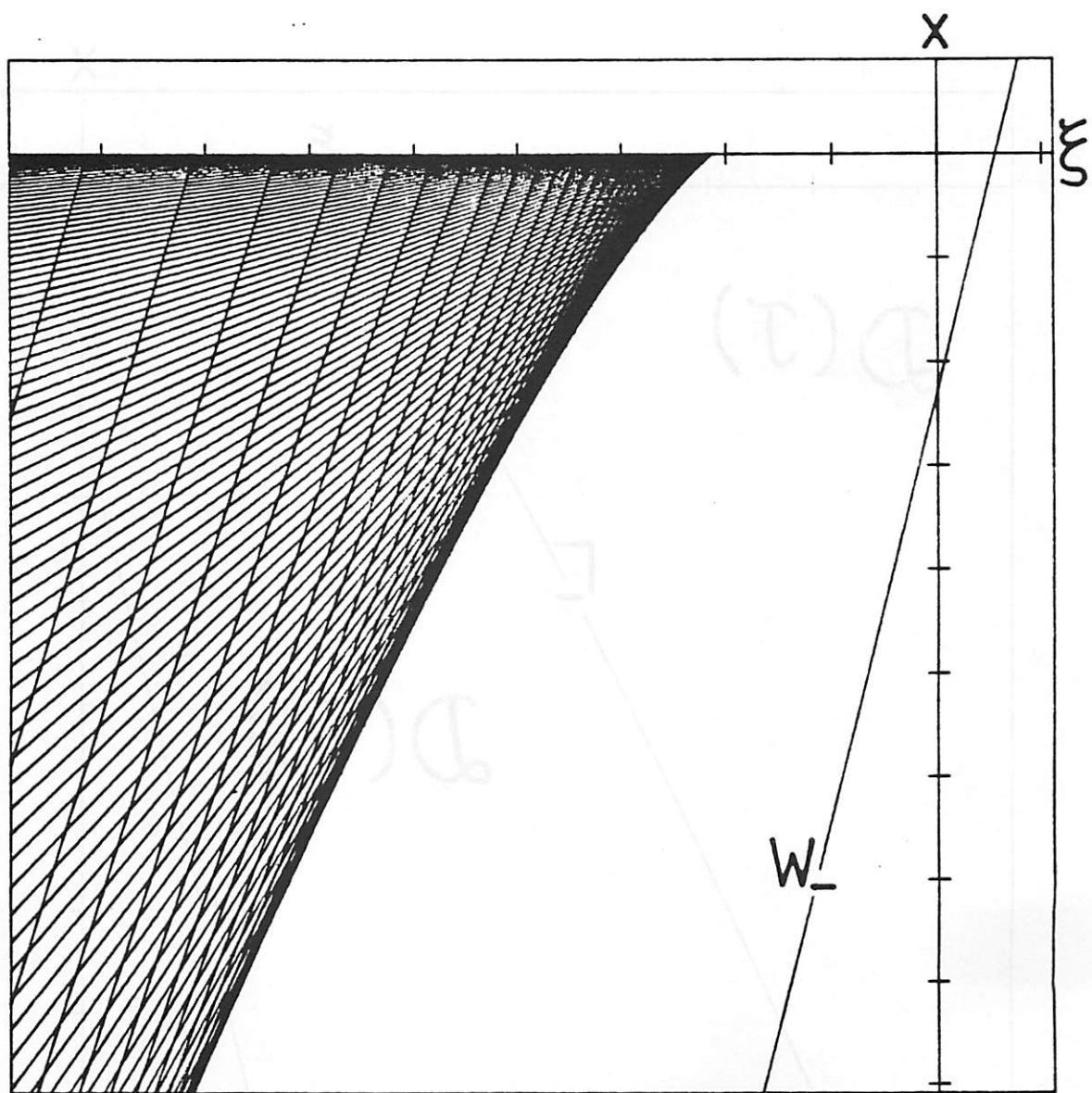
Kaklert & Chua Fig. 6



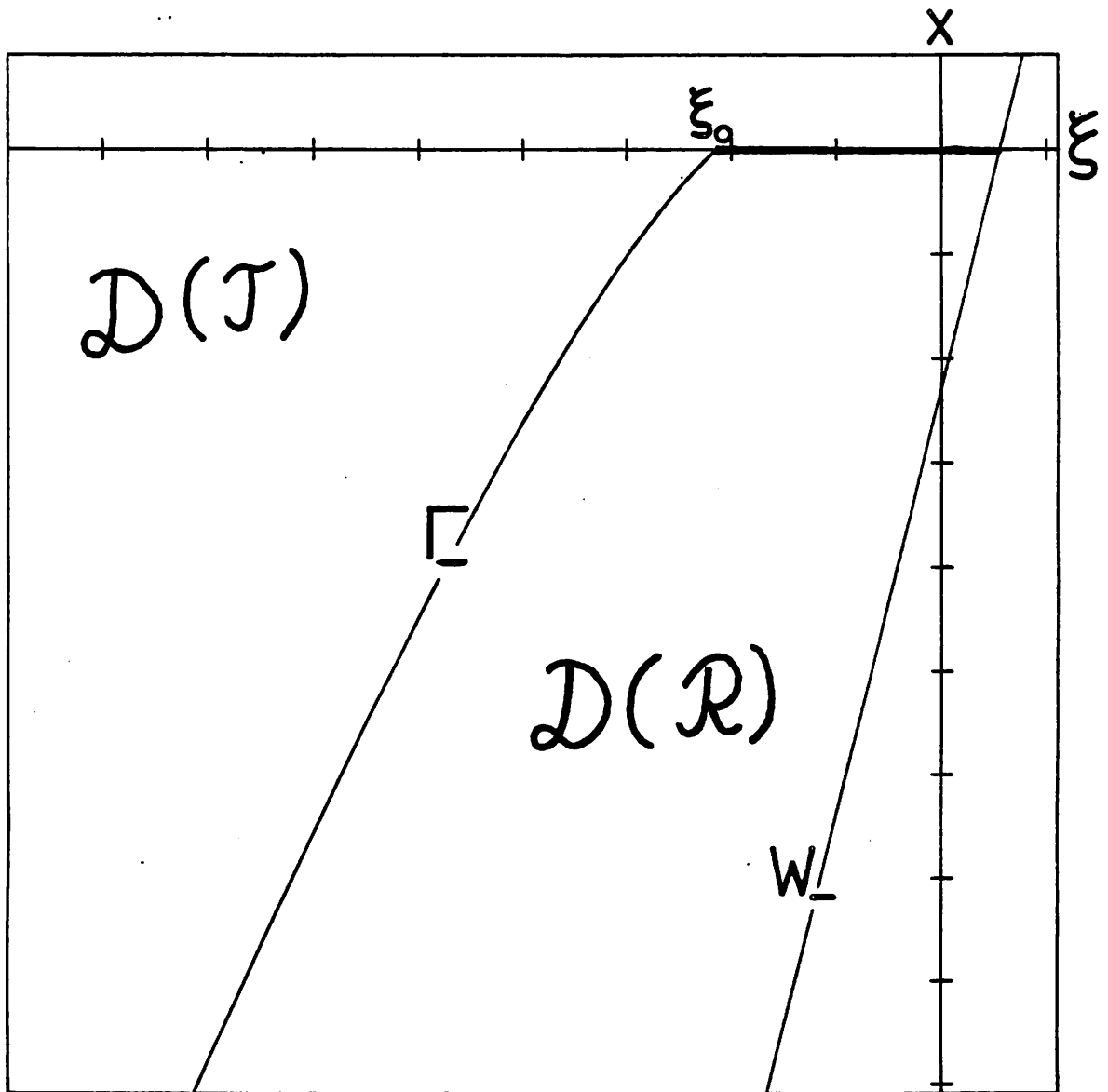
Kahlert & Chua Fig. 7



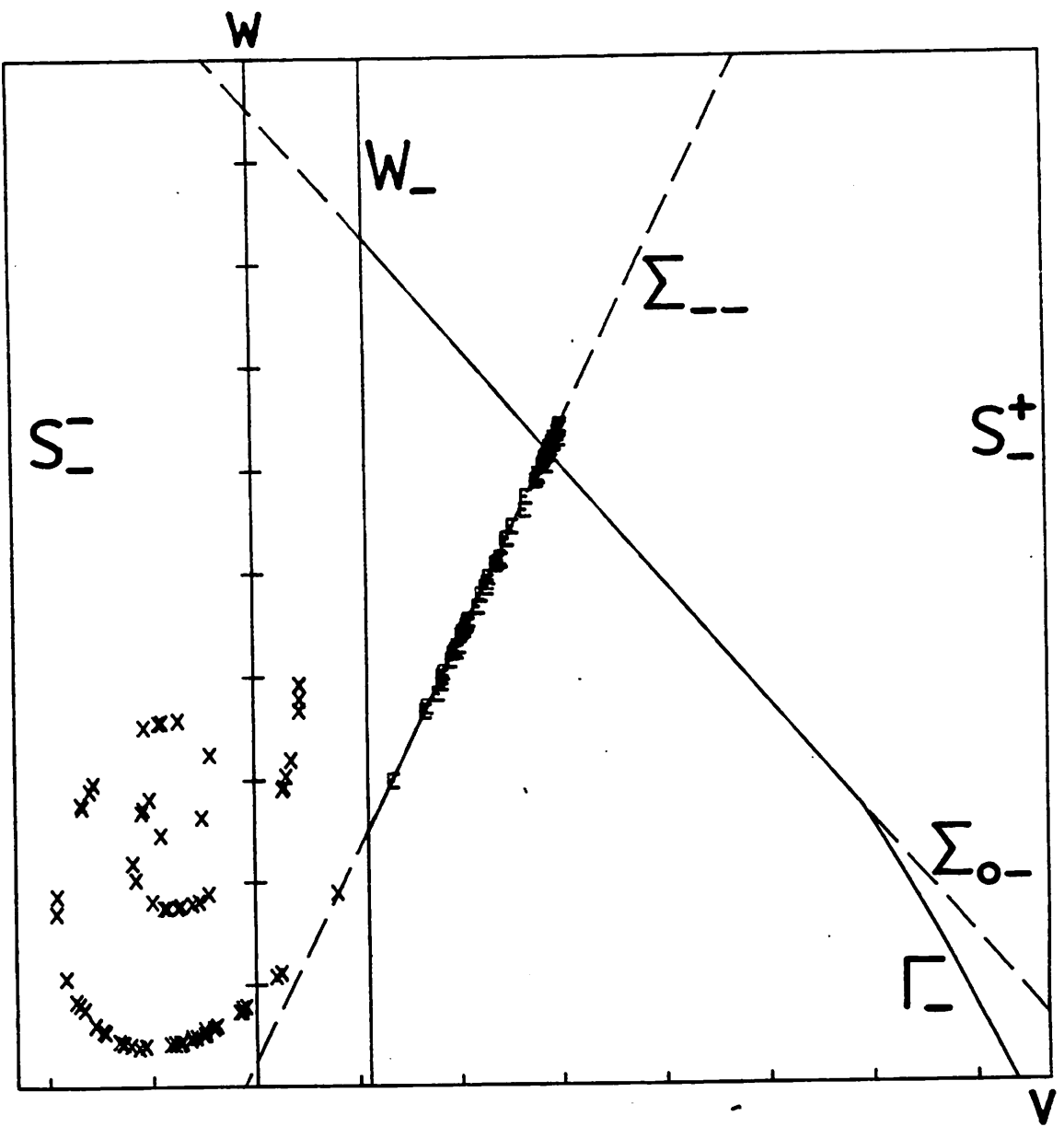
Kahlert & Chua Fig. 8



Kahlert & Chua Fig. 9



Kahler & Chua Fig. 10a



Kalant & Chua Fig 10 b, c

